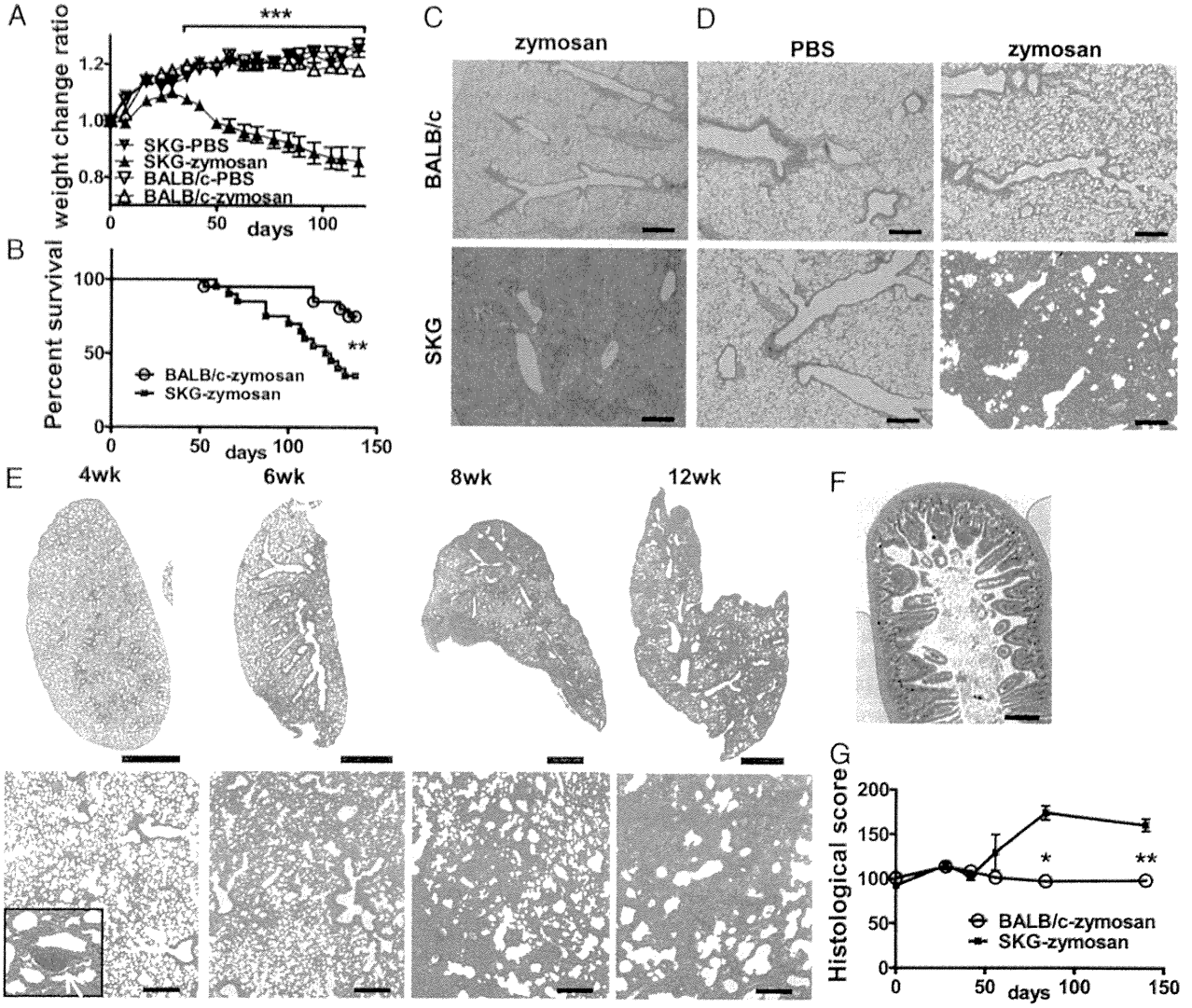

FIGURE 1. Zymosan-treated SKG mice develop chronic–progressive and severe ILD with high mortality. (**A**) The weight change ratio after i.p. injection of zymosan or PBS (PBS: $n = 5$, zymosan: $n = 30$). (**B**) The Kaplan–Meier survival analysis after injection of zymosan ($n = 20$). (**C**) H&E stain of the lung from zymosan-treated BALB/c mouse (*top*) and zymosan-treated SKG mouse (*bottom*) at 18 wk after zymosan treatment. Massive infiltrations of inflammatory cells were observed in zymosan-treated SKG mouse. Scale bar, 500 μm. (**D**) Masson's trichrome stain of the lung from PBS-treated BALB/c (*upper left*), PBS-treated SKG (*lower left*), zymosan-treated BALB/c (*upper right*), and zymosan-treated SKG (*lower right*) at 18 wk after zymosan or PBS treatment. Diffuse deposition of collagen fibers was observed in zymosan-treated SKG. Scale bar, 200 μm. (**E**) The time course of lung histology of SKG mice after zymosan injections. NSIP-like inflammatory cell infiltrations with follicular bronchiolitis (arrow) were observed in 4 and 6 wk, followed by massive infiltration of inflammatory cells in 8 and 12 wk after zymosan injections. Scale bar, 1.5 mm (*top*) and 250 μm (*bottom*). (**F**) H&E staining of small intestine from zymosan-treated SKG mouse at 18 wk after zymosan treatment. Scale bar, 200 μm. (**G**) The time course of lung histological score of zymosan-treated BALB/c or SKG mice after zymosan injections ($n = 5$). $*p < 0.05$, $**p < 0.01$, $***p < 0.001$.

SKG T cells were skewed to differentiate into GM-CSF– or IL-17A–producing cells, and they are enhanced by macrophages

Freshly isolated splenic SKG $CD4^+$ T cells contained higher proportion of both GM-CSF–producing T cells and IL-17A–producing T cells (Fig. 4A). To compare the capacity of T cells to differentiate into IL-17A– or GM-CSF–producing T cells, FACS-sorted highly purified $CD4^+CD62L^+$ naive T cells from SKG or BALB/c mice were stimulated with anti-CD3 and anti-CD28 Abs for 5 d (neutral condition). FACS analyses of these T cells revealed that naive T cells from SKG mice differentiated into IL-17A–producing T cells or GM-CSF–producing T cells more preferentially than that from BALB/c mice (Fig. 4B). This result was confirmed by ELISA using culture supernatants of the same cells, although the difference of IL-17A concentration was not statistically significant (Fig. 4C). Moreover, SKG $CD4^+$ T cells are also prone to differentiate into IL-17A– or GM-CSF–producing T cells, even under Th1, Th2, or Th17 conditions, although there was no statistical difference between the frequency of GM-CSF–producing cells in SKG T cells and that in BALB/c T cells under the Th2 condition (Supplemental Fig. 2A, 2B). These results suggested that SKG $CD4^+$ T cells are primarily skewed to IL-17A– or GM-CSF–producing T cells both in vitro and in vivo. To further confirm these results, we cultured freshly isolated splenocytes from BALB/c or SKG mice with or without Con A, LPS, zymosan, or curdlan for 3 d to mimic in vivo conditions, and determined the concentration of IL-17A and GM-CSF in the supernatants by ELISA. As shown in Fig. 4D and 4E, SKG splenocytes produced higher amount of IL-17A and GM-CSF than BALB/c splenocytes

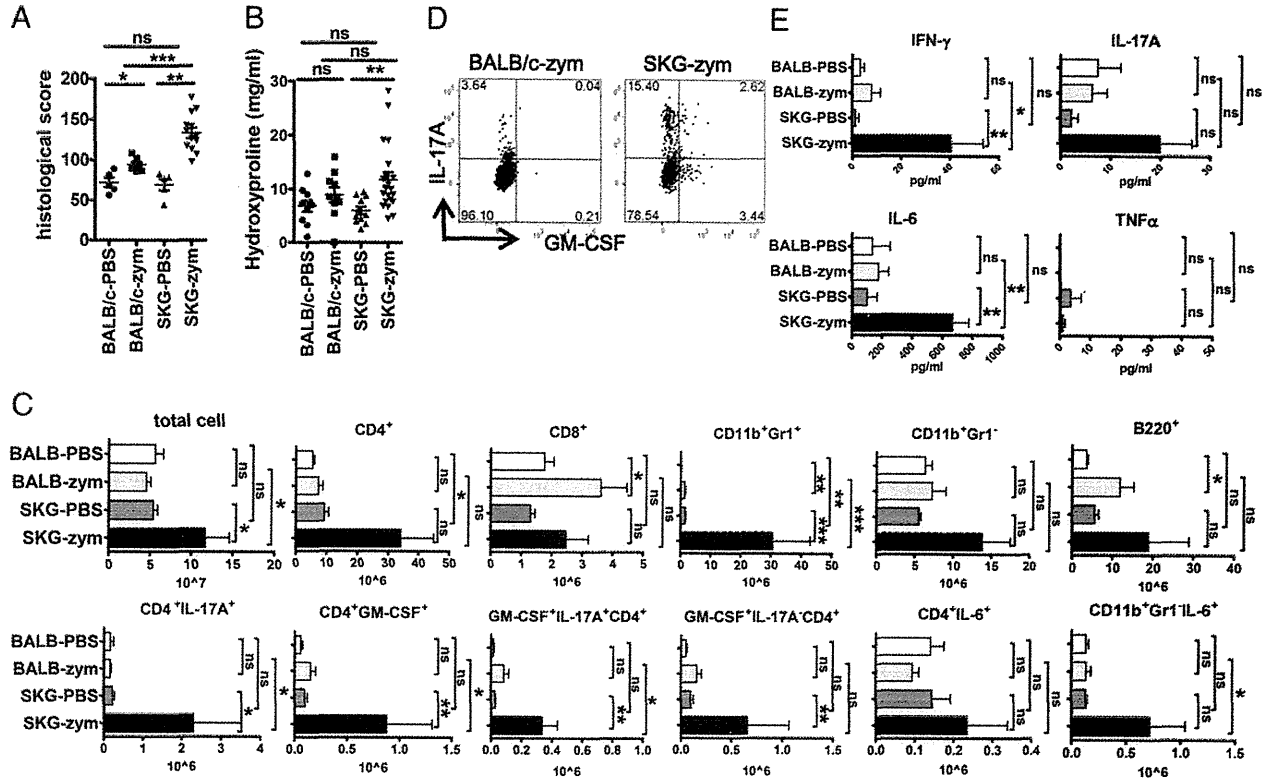

FIGURE 2. ILD in SKG mice was characterized by prominent infiltration of IL-17$^+$ CD4$^+$ T cells, GM-CSF$^+$ CD4$^+$ T cells, CD11b$^+$ Gr1$^+$ neutrophils, and pulmonary fibrosis. (**A**) Zymosan (zym)-treated SKG mice showed increased histological scores compared with zymosan (zym)-treated BALB/c mice and PBS-treated SKG mice at 18 wk after zymosan or PBS treatment (BALB/c-zym: $n = 7$, SKG-zym: $n = 13$, other groups: $n = 5$). (**B**) The concentrations of pulmonary hydroxyproline in PBS- or zymosan (zym)-treated SKG or BALB/c mice at 18 wk after zymosan or PBS treatment (SKG-zym: $n = 20$, other groups: $n = 10$). (**C**) Infiltrating cell counts in the lungs at 18 wk after zymosan or PBS treatment were measured by flow cytometry of dispersed cells from enzymatic lung digests. The numbers of total cells, CD4$^+$ T cells, CD8$^+$ T cells, CD11b$^+$ Gr1$^+$ neutrophils, CD11b$^+$ Gr1$^-$ macrophages/monocytes, B220$^+$ B cells, IL-17A–producing CD4$^+$ (CD4$^+$ IL-17A$^+$) T cells, GM-CSF–producing CD4$^+$ (CD4$^+$ GM-CSF$^+$) T cells, GM-CSF/IL-17A–double-producing CD4$^+$ (GM-CSF$^+$ IL-17A$^+$ CD4$^+$) T cells, GM-CSF–producing IL-17A–nonproducing CD4$^+$ (GM-CSF$^+$ IL-17A$^-$ CD4$^+$) T cells, IL-6–producing CD4$^+$ (CD4$^+$ IL-6$^+$) T cells, and IL-6–producing macrophages/monocytes (CD11b$^+$ Gr1$^-$ IL-6$^+$) were shown (BALB/c-PBS: $n = 5$, other groups: $n = 10$). (**D**) The majority of GM-CSF–producing CD4$^+$ T cells infiltrating in the lung of zymosan-treated SKG mouse were IL-17A–nonproducing cells. CD4$^+$ T cells infiltrating in lungs of zymosan-treated BALB/c and SKG mice at 18 wk after zymosan treatment were stained for intracellular IL-17A and GM-CSF. Representative results are shown ($n = 10$). (**E**) Serum concentrations of IFN-γ, IL-17A, IL-6, and TNF-α in BALB/c or SKG mice at 18 wk after zymosan or PBS treatment (PBS: $n = 5$, zymosan: $n = 15$). $*p < 0.05$, $**p < 0.01$, $***p < 0.001$.

in response to Con A stimulation, but single stimulation by LPS, zymosan, or curdlan did not increase IL-17A or GM-CSF production in either BALB/c or SKG splenocyte cultures. However, costimulations of both T cells and non-T cells by Con A with LPS or zymosan or curdlan significantly amplified both IL-17A and GM-CSF productions. Furthermore, the concentrations of these two cytokines from SKG splenocytes were higher than that from BALB/c (Fig. 4D, 4E). These results in Fig. 4 and Supplemental Fig. 2 collectively indicate that SKG T cells differentiate into IL-17A– or GM-CSF–producing T cells more preferentially than BALB/c T cells. Although macrophages from SKG and BALB/c mice had no qualitative differences, GM-CSF promoted IL-6 and IL-1β production from them dose dependently, as shown in Fig. 3. Therefore, it appears that higher production of GM-CSF by SKG T cells promotes higher IL-6 and IL-1β production from macrophages, which in turn promotes further preferential differentiation and expansion of IL-17A– or GM-CSF–producing T cells. In conclusion, GM-CSF–secreting SKG T cells might be a key factor to exacerbate the vicious circle of IL-17A– or GM-CSF–producing T cell expansion.

Blocking of IL-17A, GM-CSF, or IL-6 signal differently modified ILD and arthritis of zymosan-treated SKG mice

We next examined the effect of blocking IL-17A, GM-CSF, or IL-6 signals on the development of ILD and arthritis in zymosan-treated SKG mice using their neutralization/blocking Abs. Each group of SKG mice received 12 weekly i.p. injections of either anti–IL-17A Ab, anti–GM-CSF Ab, anti–IL-6R Ab, or their isotype control Abs from the day of zymosan injection. Another group of SKG mice received 12 weekly i.p. injections of PBS instead of mAbs after zymosan injection as a control of isotype Abs, and showed that there was no statistical difference among weekly PBS-treated SKG group and all the isotype Ab-treated SKG groups in the weight change ratio, histological score, or pulmonary hydroxyproline level, indicating that these isotype control Abs are not pathogenic on their own (Supplemental Fig. 3). As shown in Fig. 5, GM-CSF neutralization completely prevented the weight loss (Fig. 5A, *middle*) and inhibited the progression of arthritis in zymosan-treated SKG mice (Fig. 5B, *middle*). In contrast, IL-17A neutralization did not suppress the weight loss but slightly suppressed the progression of arthritis in zymosan-treated SKG mice (Fig. 5A, 5B, *left*). Blocking of IL-6 signal weakly suppressed the weight loss (but it was not statistically significant) but did not affect the progression of arthritis in zymosan-treated SKG mice (Fig. 5A, 5B, *right*). Histological analysis after 12 injections revealed that GM-CSF neutralization and IL-6 signal blocking inhibited ILD progression in zymosan-treated SKG mice; however, IL-17A neutralization did not at all (Fig. 5C, 5D). The estimation of fibrosis by hydroxyproline confirmed these histological findings

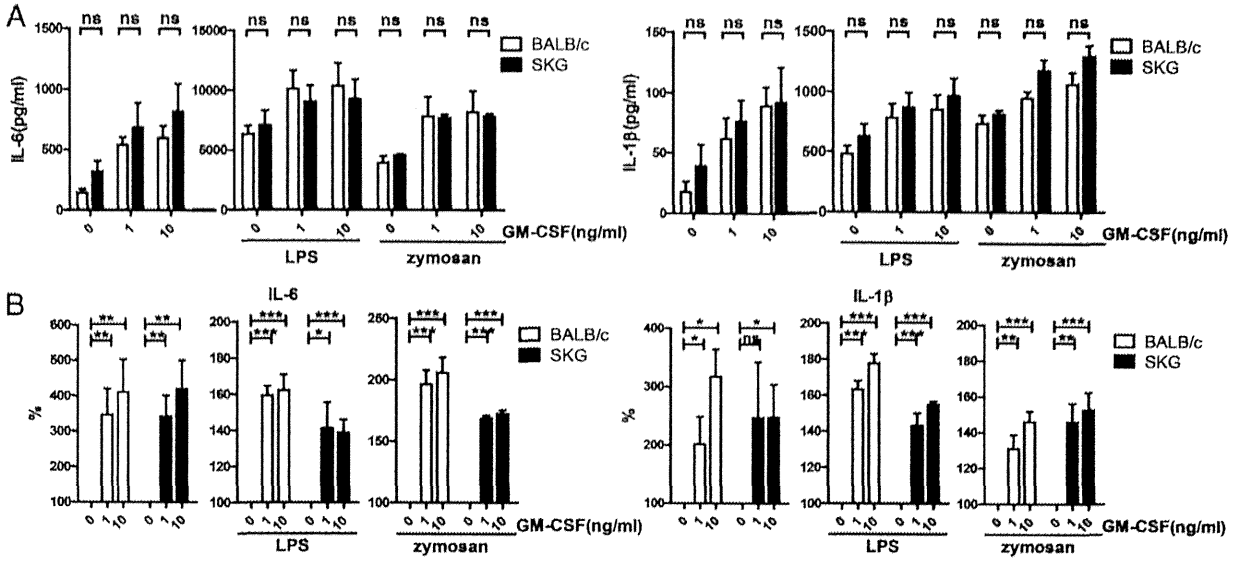

FIGURE 3. Cytokine production from macrophages of SKG mice was equivalent to that of BALB/c mice and enhanced by GM-CSF. (**A**) Peritoneal CD11b$^+$ macrophages were cultured for 3 d with or without 100 ng/ml LPS or 1 μg/ml zymosan in the presence of GM-CSF at indicated doses. IL-6 and IL-1β in the supernatant were measured by ELISA ($n = 5$). (**B**) Percentage of changes of cytokine concentrations shown in (A) from cultures without GM-CSF ($n = 5$). $*p < 0.05$, $**p < 0.01$, $***p < 0.001$.

(Fig. 5E). These results demonstrated that IL-17A, GM-CSF, and IL-6 have different roles in ILD and arthritis of zymosan-treated SKG mice, and that GM-CSF and IL-6 were more potent molecular targets to treat ILD in this mouse than IL-17A.

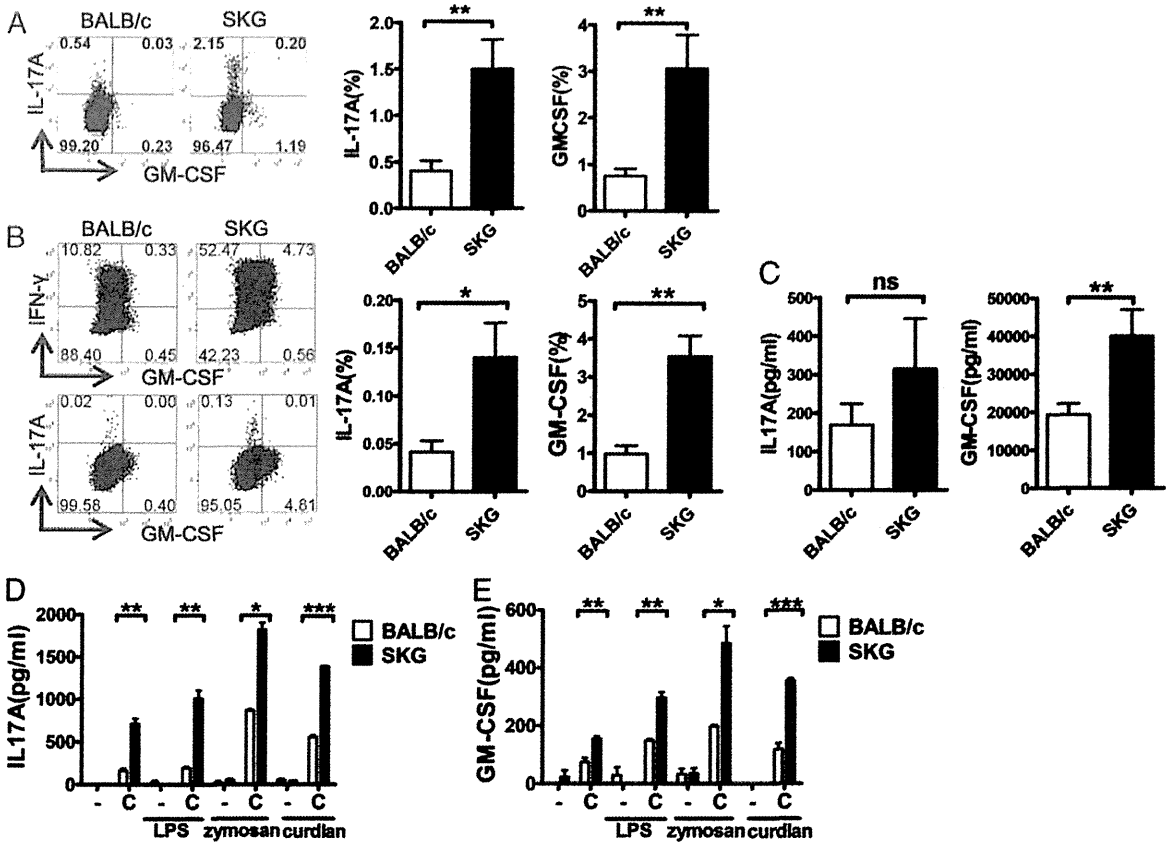

FIGURE 4. SKG T cells were skewed to differentiate into IL-17A– and GM-CSF–producing cells. (**A**) Freshly isolated BALB/c or SKG splenic CD4$^+$ T cells were stained for intracellular IL-17A and GM-CSF. Representative results are shown ($n = 8$). (**B** and **C**) FACS-sorted CD4$^+$ CD62L$^+$ naive T cells of SKG and BALB/c mice were cultured under the stimulation of anti-CD3/28 Abs. At day 5, cultured cells were analyzed by FACS (B), or restimulated with PMA/ionomycin for 24 h, and the concentrations of IL-17A and GM-CSF in the culture supernatants were determined by ELISA (C). Representative results are shown ($n = 5$). (**D** and **E**) Freshly isolated BALB/c or SKG splenocytes were cultured with or without Con A (C), LPS, zymosan, or curdlan for 3 d, and the concentrations of IL-17A (D) and GM-CSF (E) in the supernatants were measured by ELISA ($n = 3$). $*p < 0.05$, $**p < 0.01$, $***p < 0.001$.

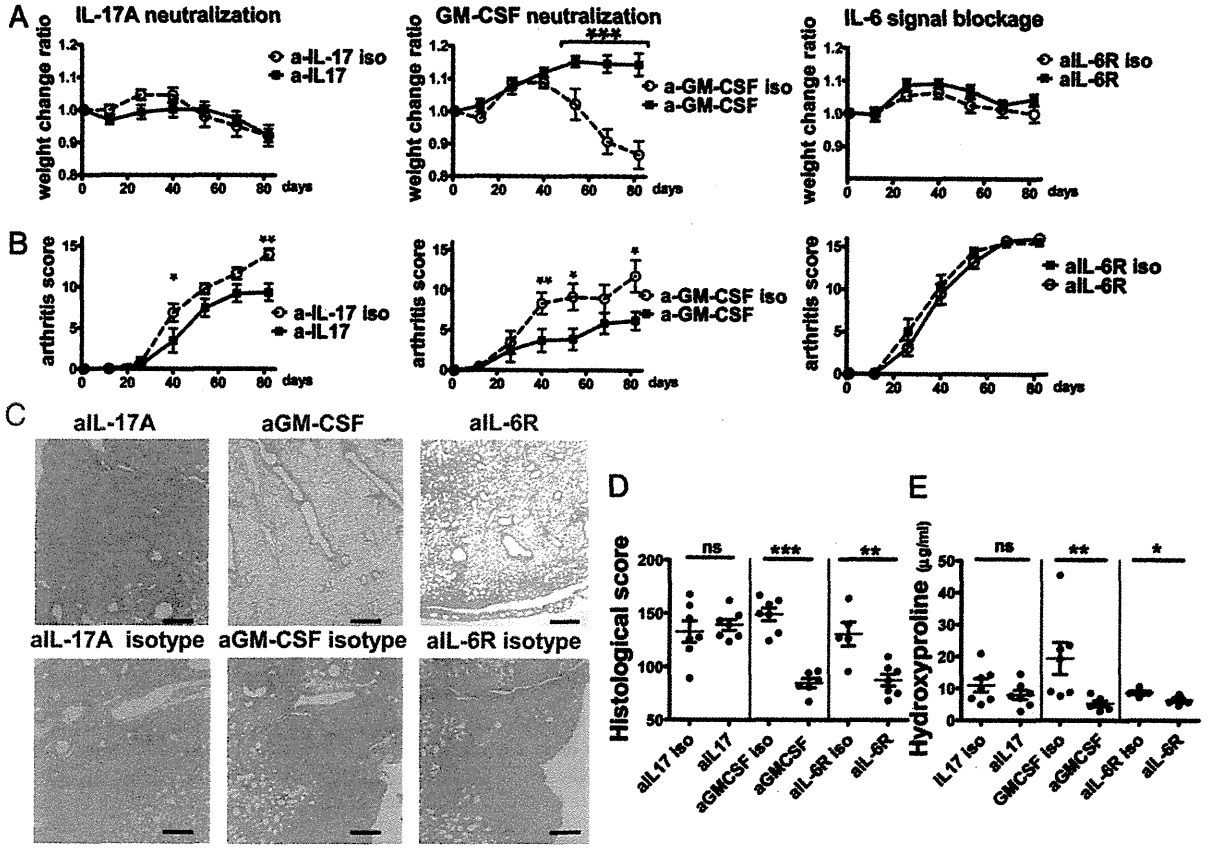

FIGURE 5. GM-CSF neutralization inhibited the development of ILD in SKG mice. (**A** and **B**) Weight change ratio (A) and arthritis score (B) of SKG mice that received a single i.p. injection of zymosan and 12 weekly i.p. injections of anti–IL-17A Ab (*left*), anti–GM-CSF Ab (*middle*), anti–IL-6R Ab (*right*), or their isotype Abs from the day of zymosan injections (anti–IL-6R isotype: $n = 5$, other groups: $n = 7$). (**C**) H&E stain of the lung from anti–IL-17A Ab (*upper left*), anti–GM-CSF Ab (*upper middle*), anti–IL-6R Ab (*upper right*), or their isotype Abs (*bottom*) injected SKG mouse at 12 wk after zymosan treatment. Scale bar, 500 μm. (**D**) Histological score of anti–IL-17A Ab, anti–GM-CSF Ab, anti–IL-6R Ab, or their isotype Ab injected SKG mice at 12 wk after zymosan treatment (anti–IL-6R isotype: $n = 5$, other groups: $n = 7$). (**E**) The concentrations of pulmonary hydroxyproline in anti–IL-17A Ab, anti–GM-CSF Ab, anti–IL-6R Ab, or their isotype Abs injected SKG mice at 12 wk after zymosan treatment (anti–IL-6R isotype: $n = 5$, other groups: $n = 7$). $^*p < 0.05$, $^{**}p < 0.01$, $^{***}p < 0.001$.

To examine the completeness of IL-17A or GM-CSF neutralization, the serums of Ab-injected mice were diluted to indicated concentrations and added to the 500 pg/ml IL-17A– or GM-CSF–containing sample. The concentration of IL-17A (Supplemental Fig. 4A) and GM-CSF (Supplemental Fig. 4B) in the samples was reduced serum dose dependently and revealed that those serums contained sufficient Abs to neutralize targeted cytokines even at the endpoint. Moreover, the concentration of anti-rat IgG Ab in the serums of anti–GM-CSF Ab or its isotype Ab-injected mice was negligible in most of them (Supplemental Fig. 4C). These data confirmed that IL-17A or GM-CSF neutralization worked completely in this study without induction of Abs against the injected neutralization Abs.

GM-CSF neutralization strongly blocked infiltration of IL-17A– and GM-CSF–producing CD4$^+$ T cells and CD11b$^+$ Gr1$^+$ neutrophils in the lung of zymosan-treated SKG mice

We next measured serum cytokines and fractionations of lung-infiltrating cells of treated mice in Fig. 5. As shown in Fig. 6A, GM-CSF neutralization reduced the serum IFN-γ, IL-17A, IL-6, and TNF-α, but, among them, only IL-6 decreased significantly. In contrast, IL-17A neutralization obviously shut off the serum IL-17A, but serum IL-6 was not decreased. In contrast, by blocking the IL-6 signal, all of these cytokines did not significantly change when compared with its isotype Ab-treated mice. IL-4 and GM-CSF were not detected in all groups (data not shown). These data suggested that IL-17A is dispensable for the progression of this ILD. As shown in Fig. 6B, flow cytometric analysis of infiltrating cells in the lungs revealed significant decrease of total cell counts in anti–GM-CSF Ab-treated mice and relative decrease in anti–IL-6R Ab-treated mice; however, there was no decrease in anti–IL-17A Ab-treated mice. These findings well correlated with the data in Fig. 5. Moreover, GM-CSF neutralization significantly decreased the numbers of infiltrated total CD4$^+$ T cells (especially IL-17A–, GM-CSF–, and IL-6–producing CD4$^+$ T cells), CD11b$^+$ Gr1$^+$ neutrophils, and IL-6–producing CD11b$^+$ Gr1$^-$ macrophages/monocytes. In contrast, blocking of IL-6 signal decreased CD11b$^+$ Gr1$^+$ neutrophils only among these cell populations, and IL-17A neutralization did not decrease any of them. Notably, the number of GM-CSF$^+$ IL-17A$^-$ CD4$^+$ cells, which are major GM-CSF–producing cells, was decreased by GM-CSF neutralization and partly by blocking of IL-6 signal, but that of GM-CSF$^+$ IL-17A$^+$ cells was decreased only by GM-CSF neutralization. These results demonstrated that the most potent molecular target to treat ILD in this mouse was GM-CSF, and that the infiltration of IL-17A–, GM-CSF–producing CD4$^+$ T cells, IL-6–producing CD11b$^+$ Gr1$^-$ macrophages/monocytes, and CD11b$^+$ Gr1$^+$ neutrophils progressed secondary to GM-CSF upregulation in the development of ILD in zymosan-treated SKG mice and can be inhibited by GM-CSF neutralization.

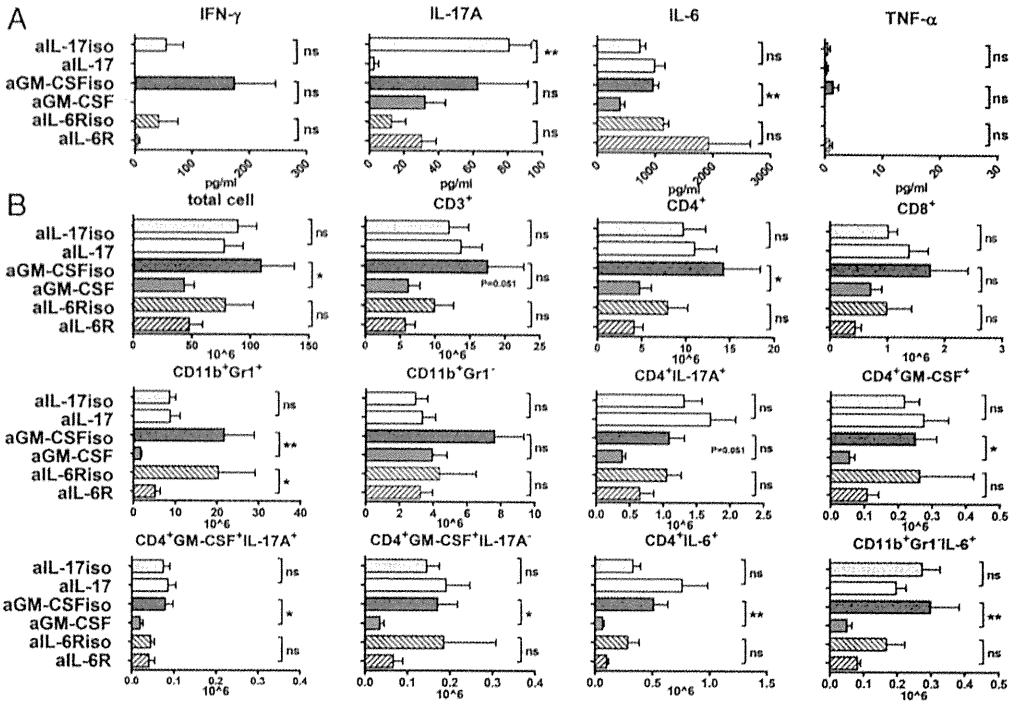

FIGURE 6. GM-CSF neutralization inhibited infiltration of IL-17A$^+$ CD4$^+$ T cells, GM-CSF$^+$ CD4$^+$ T cells, and CD11b$^+$ Gr1$^+$ neutrophils into the lung. (**A**) Serum concentrations of IFN-γ, IL-17A, IL-6, and TNF-α in anti–IL-17A Ab, anti–GM-CSF Ab, anti–IL-6R Ab, or their isotype Abs injected SKG mice at 12 wk after zymosan treatment (anti–IL-6R isotype: $n = 5$, other groups: $n = 7$). (**B**) Infiltrating cell counts in the lungs were measured by flow cytometry of dispersed cells from enzymatic lung digests at 12 wk after zymosan treatment. The numbers of total cells, CD3$^+$ T cells, CD4$^+$ T cells, CD8$^+$ T cells, CD11b$^+$ Gr1$^+$ neutrophils, CD11b$^+$ Gr1$^-$ macrophages/monocytes, IL-17A–producing CD4$^+$ (CD4$^+$ IL-17A$^+$) T cells, GM-CSF–producing CD4$^+$ (CD4$^+$ GM-CSF$^+$) T cells, GM-CSF/IL-17A–double-producing CD4$^+$ (GM-CSF$^+$ IL-17A$^+$ CD4$^+$) T cells, GM-CSF–producing IL-17A–nonproducing CD4$^+$ (GM-CSF$^+$ IL-17A$^-$ CD4$^+$) T cells, IL-6–producing CD4$^+$ (CD4$^+$ IL-6$^+$) T cells, and IL-6–producing macrophages/monocytes (CD11b$^+$ Gr1$^-$ IL-6$^+$) were shown (anti–IL-6R isotype: $n = 5$, other groups: $n = 7$). $*p < 0.05$, $**p < 0.01$.

Treatment by GM-CSF neutralization after the onset of ILD reduced the severity of ILD in zymosan-treated SKG mice

We next analyzed the effect of GM-CSF neutralization after the onset of ILD in zymosan-treated SKG mice. As the histological score of zymosan-treated SKG mice started to increase from the sixth week after zymosan injection (Fig. 1E), each group of SKG mice received six weekly i.p. injections of either anti–GM-CSF Ab or its isotype Ab from the sixth week after zymosan injection. GM-CSF neutralization prevented the weight loss (Fig. 7A) and inhibited the progression of arthritis in zymosan-treated SKG mice (Fig. 7B). Moreover, as shown in Fig. 7C and 7D, GM-CSF neutralization inhibited the progression of ILD in zymosan-treated SKG mice even after the onset of ILD. These results suggested the high potential of GM-CSF neutralization as a therapeutic strategy for severe CTD-ILD in humans (Fig. 8).

Discussion

We described whole features of ILD in zymosan-treated SKG mice and showed that this model is a valuable animal model for CTD-ILD in terms of the chronicity (not self limiting), long time course (5–6 mo), and severity. The most common histological type of CTD-ILD is NSIP (27), and the ILD in this mouse shared many characteristics with NSIP in CTD-ILD in the early phase in terms of the temporally uniform interstitial cellular infiltration and fibrosis, which started in peribronchovascular lesion without honeycombing or fibroblastic foci. Furthermore, it accompanied follicular bronchiolitis, which is one of the characteristics of CTD-ILD (26). Moreover, in the later phase, the ILD in this mouse showed massive infiltration of inflammatory cells within both peribronchiolar and alveolar spaces. It is also known that a combination of different histological patterns and the progressive exacerbation is also pathognomonic and quite frequent in CTD-ILD (27). Therefore, the histological characteristics of ILD in this mouse could be extrapolated to that of severe CTD-ILD. The underlying mechanisms of CTD-ILD development remain poorly understood because of the invasiveness of analyzing procedure such as BAL or open lung biopsy. CD8$^+$ T cells (30, 31), as well as some subtypes of CD4$^+$ T cells, including Th2, regulatory T cells, and Th17 cells (32, 33), and neutrophils (5–8) are reported as contributors of pulmonary fibrosis. However, in contrast with idiopathic pulmonary fiborosis, CTD-ILD is often characterized by a clearer response to immunosuppression, indicating that autoimmune/inflammatory mechanisms play a more significant and central role than fibrosis in CTD-ILD pathogenesis (27, 34). Analyses of alveolitis using BAL fluid showed accumulation of neutrophils with or without increased percentages of T cells in the small airways of CTD-ILD (4, 5), and neutrophils were reported as important effector cells and associated with poor outcome of CTD-ILD (5–8). The CD4/CD8 ratios in BAL fluid of CTD-ILD patients vary with reports (30, 35–39); however, a previous report showed that correlation between CD4/CD8 ratios in lung tissue and CD4/CD8 ratios in BAL fluid was weak and that CD4/CD8 ratio in BAL fluid would rather reflect the extent of fibrosis (40). In contrast, in histological analyses, increased number of CD4$^+$ T cells in lung tissue of open lung biopsy was reported as characteristics of CTD-ILD (9). Previous reports showed that CD4$^+$ T cells and B cells were observed inside and around lymphoid follicles and in the thick fibrotic wall of reconstructed alveoli with fibrosis, and CD8$^+$ T cells were diffusely distributed especially in

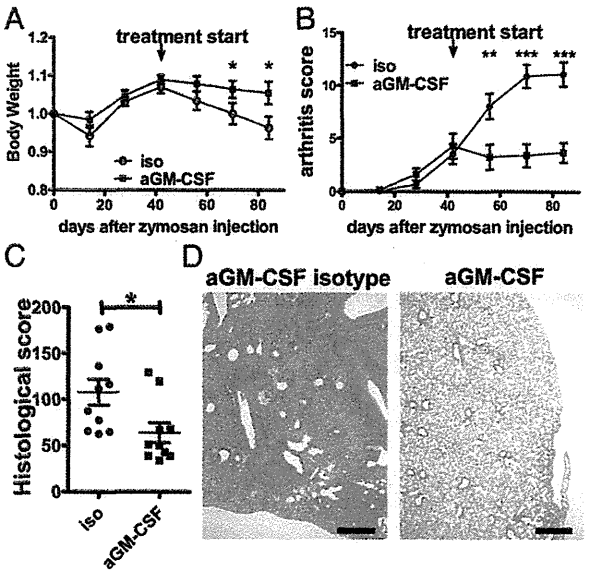

FIGURE 7. GM-CSF neutralization inhibited the progression of ILD even after the onset of ILD. (**A** and **B**) Weight change ratio (A) and arthritis score (B) of SKG mice that received a single i.p. injection of zymosan followed by six weekly i.p. injections of anti–GM-CSF Ab (*left*) or its isotype Ab from the sixth week after zymosan injections (n = 10). (**C**) Histological scores of SKG mice given six anti–GM-CSF Ab or isotype Ab weekly injections at 12 wk after zymosan injection (n = 10). (**D**) H&E stain of the lung from SKG mouse given six anti–GM-CSF Ab (*right*) or its isotype Ab (*left*) weekly injections at 12 wk after zymosan injection. Scale bar, 500 μm. $*p < 0.05$, $**p < 0.01$, $***p < 0.001$.

relatively thin alveoli in CTD-ILD patients, suggesting that $CD4^+$ and B cells initiate and operate cell-mediated humoral and immune mechanisms and $CD8^+$ T cells and neutrophils cause lung injury in the CTD-ILD (37, 40). By cytological analysis, ILD in SKG mice was characterized by the increased infiltration of $CD4^+$ T cells and neutrophils. Therefore, these data also indicated the similarity of CTD-ILD and ILD in zymosan-treated SKG mice and that $CD4^+$ T cells as well as neutrophils are critical for the development of both of them. Therefore, ILD in this mouse can be a suitable model of severe CTD-ILD and is very useful to analyze the mechanisms and the effects of the therapeutic interventions to treat them.

SKG arthritis is known to be mediated by Th17 cells (13), but the mechanisms underlying the progression of ILD are yet to be clarified. In this study, we showed that high potential of SKG T cells to produce GM-CSF produced a different outcome between zymosan-treated SKG and BALB/c. GM-CSF was reported to upregulate TLR2, TLR4, and CD14 expression (41–43) and boost IL-6 and IL-1β production from macrophages (41, 44, 45). Although serum concentration of GM-CSF in zymosan-treated SKG mice was very low and could not be detected by ELISA, we showed that GM-CSF could enhance the production of IL-6 and IL-1β by macrophages even at a low concentration (Fig. 3). In addition, GM-CSF itself is a strong inducer of neutrophil infiltration (46). Previous reports showed that overexpression of GM-CSF led to severe neutrophil and macrophage infiltration in multiple tissues, including lung (47), and, as we showed, GM-CSF neutralization significantly inhibited the neutrophil infiltration into the lung of zymosan-treated SKG mice (Fig. 6B). These results indicated that GM-CSF essentially contributed to the progression of ILD in zymosan-treated SKG mice both directly and indirectly.

GM-CSF is known as one of the Th17 cytokines; however, it is not exclusively produced by Th17 cells, but also by other T cell subsets, including $CD8^+$ T cells. The number of GM-CSF–producing $CD8^+$ T cells also increased in both zymosan-treated BALB/c and zymosan-treated SKG mice (Supplemental Fig. 4D). However, the contribution of GM-CSF–producing $CD8^+$ T cells to the development of ILD seems to be small, for the number of GM-CSF–producing $CD8^+$ T cells is about one-tenth of that of GM-CSF–producing $CD4^+$ T cells (Fig. 2C) in zymosan-treated SKG mice and is equivalent to that in zymosan-treated BALB/c mice. These results reinforced that GM-CSF$^+$ IL-17A$^-$ $CD4^+$ T cells are main effector cells in this model.

IL-17A is also known as a strong inducer of neutrophil infiltration (48), but IL-17A neutralization was not effective to prevent ILD in this mouse. Considering the previous report that no morphological change was found in the lungs of IL-17–overexpressing mice (49) and that serum IL-17A was almost completely diminished in anti–IL-17A–injected group and was not in anti–GM-CSF Ab- or anti–IL-6R Ab-injected group, IL-17A seemed not to be essential for the development of this ILD. In addition, there was

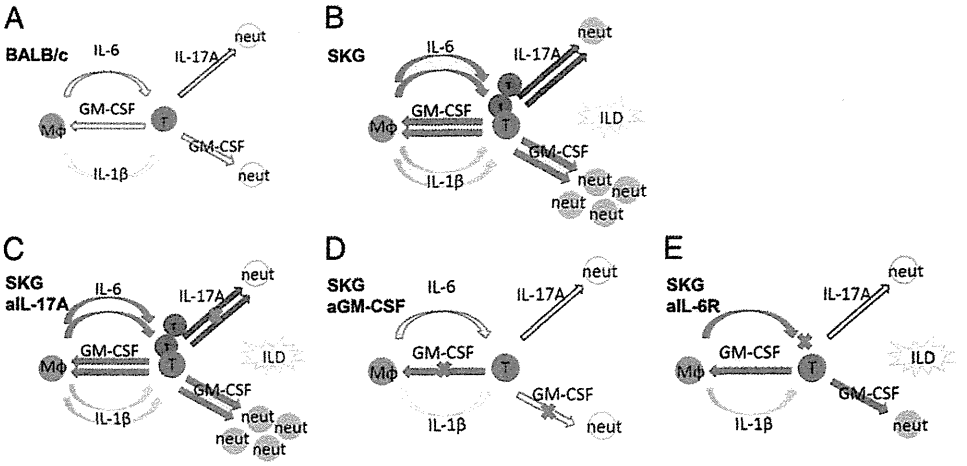

FIGURE 8. Models of the role of GM-CSF in the development of ILD in SKG mice. (**A**) T cells of zymosan-treated BALB/c mice produce lower amount of GM-CSF or IL-17A in response to macrophage stimulation, and the vicious circle of IL-17A– and GM-CSF–producing T cell expansion is not exacerbated. (**B**) T cells of zymosan-treated SKG mice preferentially produce higher amount of GM-CSF, which stimulates cytokine production of macrophages, and resulted in exacerbation of vicious circle of IL-17A– and GM-CSF–producing T cell expansion. (**C–E**) A model of IL-17A neutralization (C), GM-CSF neutralization (D), and anti–IL-6R Ab (E) treatment in zymosan-treated SKG mice.

no difference between zymosan-treated BALB/c and zymosan-treated SKG mice in the serum IL-17AF heterodimer or IL-17F homodimer, the other IL-17 family members secreted by $CD4^+$ T cells and having similar function (48) (Supplemental Fig. 4E), indicating they are not important to the pathogenesis of this ILD either.

By contrast, anti–IL-6R Ab treatment resulted in partial amelioration of ILD in this mouse. Blocking of IL-6 signal reduced the number of GM-CSF^+ IL-$17A^-$ $CD4^+$ T cells to some extent but not that of GM-CSF^+ IL-$17A^+$ $CD4^+$ T cells, although GM-CSF neutralization reduced both of them (Fig. 6B). These differences may be the cause of partial inhibition of ILD by blocking of IL-6 signal. In addition, considering that anti–IL-6R Ab or its isotype Ab-injected mice received higher amount of Ig than anti–IL-17A or anti–GM-CSF Ab-injected groups, higher Ig dosages themselves may have some curative effects as reported effect of high-dose i.v. Ig therapy (50). In fact, the severity of ILD and weight loss in the isotype Ab of anti–IL-6R–treated group seemed milder than that of anti–IL-17A isotype or anti–GM-CSF isotype Ab-treated groups, although there was no statistical difference (Fig. 5A, 5D, 5E, Supplemental Fig. 3).

In summary, we found that GM-CSF plays a key role by enhancing IL-6 and IL-1β production from zymosan-activated macrophages to promote the differentiation of IL-17A– or GM-CSF–producing T cells. Moreover, GM-CSF enhances granulopoiesis and neutrophil infiltration (Fig. 8A, 8B). Therefore, GM-CSF neutralization strongly inhibited the progression of ILD in this mouse by blocking both positive feedback loop of IL-17A– and GM-CSF–producing T cell differentiation and the neutrophil infiltration induced by GM-CSF itself (Fig. 8D). IL-17A neutralization failed to ameliorate this ILD, indicating that IL-17A is not a key molecule to the progression of this ILD (Fig. 8C). Blocking of IL-6 signal resulted in partial inhibition of this ILD, indicating that it partially suppressed the differentiation of IL-17– and GM-CSF–producing T cells, and then neutrophil infiltration in lung (Fig. 8E).

It is known that auto-Ab to GM-CSF is responsible for the development of pulmonary alveolar proteinosis (PAP) (51), and GM-CSF–deficient mice develop abnormal lung virtually indistinguishable from human PAP (52). However, only trace amounts of GM-CSF are needed for lung homeostasis, and neutralizing GM-CSF with Abs in mice has no demonstrated adverse reactions, indicating its wide therapeutic index (53). In fact, there was no evidence for alveolar proteinosis in anti–GM-CSF Ab-treated mice such as foamy alveolar macrophages in a distinctive background of eosinophilic, granular, periodic acid-Schiff positive material filling alveoli (51) (Supplemental Fig. 4F). Therefore, neutralization/blocking Abs are a useful approach and can easily receive clinical applications. Now, Mavrilimumab, anti–GM-CSF receptor α Ab, is being developed, and a phase II study in subjects with rheumatoid arthritis patients is reported to have significant efficacy and no serious adverse events, including PAP (54). Regarding the fact that neutralization of GM-CSF ameliorated ILD in SKG mice even after the onset of ILD, it can provide a useful therapeutic strategy in CTD-ILD in humans.

In conclusion, we described that zymosan-treated SKG mice develop chronic–progressive and lethal ILD over several months, and ILD of this mouse shared many characteristics with severe CTD-ILD. Therefore, this ILD might be a useful mouse model for elucidating the underlying mechanism and devising effective treatment of severe CTD-ILD. Furthermore, we found that GM-CSF played a pivotal role in the pathogenesis of ILD in this mouse, and that neutralization of GM-CSF has great therapeutic potential. Because it is almost impossible to examine the pathology in life-threatening severe CTD-ILD in humans, further elucidation of the molecular mechanisms of ILD in this mouse would help in devising preventive or curative strategies for it.

Acknowledgments

We thank Kensaku Aihara (Department of Respiratory Medicine, Graduate School of Medicine, Kyoto University) for technical support on hydroxyproline measurement, Aya Miyagawa-Hayashino (Department of Diagnostic Pathology, Kyoto University Hospital) for pathological evaluation, and Sonoko Nagai (Department of Respiratory Medicine, Graduate School of Medicine, Kyoto University) for critical reading.

Disclosures

The authors have no financial conflicts of interest.

References

1. Castelino, F. V., and J. Varga. 2010. Interstitial lung disease in connective tissue diseases: evolving concepts of pathogenesis and management. *Arthritis Res. Ther.* 12: 213.
2. Katzenstein, A. L., and J. L. Myers. 1998. Idiopathic pulmonary fibrosis: clinical relevance of pathologic classification. *Am. J. Respir. Crit. Care Med.* 157: 1301–1315.
3. Parra, E. R., G. S. Noleto, L. J. Tinoco, and V. L. Capelozzi. 2008. Immunophenotyping and remodeling process in small airways of idiopathic interstitial pneumonias: functional and prognostic significance. *Clin. Respir. J.* 2: 227–238.
4. Wallaert, B. 1990. Subclinical alveolitis in immunologic systemic disorders. *Lung* 168: 974–983.
5. Manganelli, P., F. Salaffi, and A. Pesci. 1997. Clinical and subclinical alveolitis in connective tissue diseases assessed by bronchoalveolar lavage. *Semin. Arthritis Rheum.* 26: 740–754.
6. Garcia, J. G., N. Parhami, D. Killam, P. L. Garcia, and B. A. Keogh. 1986. Bronchoalveolar lavage fluid evaluation in rheumatoid arthritis. *Am. Rev. Respir. Dis.* 133: 450–454.
7. Garcia, J. G., H. L. James, S. Zinkgraf, M. B. Perlman, and B. A. Keogh. 1987. Lower respiratory tract abnormalities in rheumatoid interstitial lung disease: potential role of neutrophils in lung injury. *Am. Rev. Respir. Dis.* 136: 811–817.
8. Marie, I., E. Hachulla, P. Chérin, S. Dominique, P. Y. Hatron, M. F. Hellot, B. Devulder, S. Herson, H. Levesque, and H. Courtois. 2002. Interstitial lung disease in polymyositis and dermatomyositis. *Arthritis Rheum.* 47: 614–622.
9. Turesson, C., E. L. Matteson, T. V. Colby, Z. Vuk-Pavlovic, R. Vassallo, C. M. Weyand, H. D. Tazelaar, and A. H. Limper. 2005. Increased CD4+ T cell infiltrates in rheumatoid arthritis-associated interstitial pneumonitis compared with idiopathic interstitial pneumonitis. *Arthritis Rheum.* 52: 73–79.
10. Moore, B., W. E. Lawson, T. D. Oury, T. H. Sisson, K. Raghavendran, and C. M. Hogaboam. 2013. Animal models of fibrotic lung disease. *Am. J. Respir. Cell Mol. Biol.* 49: 167–179.
11. Sakaguchi, N., T. Takahashi, H. Hata, T. Nomura, T. Tagami, S. Yamazaki, T. Sakihama, T. Matsutani, I. Negishi, S. Nakatsuru, and S. Sakaguchi. 2003. Altered thymic T-cell selection due to a mutation of the ZAP-70 gene causes autoimmune arthritis in mice. *Nature* 426: 454–460.
12. Keith, R. C., J. L. Powers, E. F. Redente, A. Sergew, R. J. Martin, A. Gizinski, V. M. Holers, S. Sakaguchi, and D. W. Riches. 2012. A novel model of rheumatoid arthritis-associated interstitial lung disease in SKG mice. *Exp. Lung Res.* 38: 55–66.
13. Hirota, K., M. Hashimoto, H. Yoshitomi, S. Tanaka, T. Nomura, T. Yamaguchi, Y. Iwakura, N. Sakaguchi, and S. Sakaguchi. 2007. T cell self-reactivity forms a cytokine milieu for spontaneous development of IL-17+ Th cells that cause autoimmune arthritis. *J. Exp. Med.* 204: 41–47.
14. Yoshitomi, H., N. Sakaguchi, K. Kobayashi, G. D. Brown, T. Tagami, T. Sakihama, K. Hirota, S. Tanaka, T. Nomura, I. Miki, et al. 2005. A role for fungal beta-glucans and their receptor Dectin-1 in the induction of autoimmune arthritis in genetically susceptible mice. *J. Exp. Med.* 201: 949–960.
15. Hashimoto, M., K. Hirota, H. Yoshitomi, S. Maeda, S. Teradaira, S. Akizuki, P. Prieto-Martin, T. Nomura, N. Sakaguchi, J. Köhl, et al. 2010. Complement drives Th17 cell differentiation and triggers autoimmune arthritis. *J. Exp. Med.* 207: 1135–1143.
16. Zhang, Y., G. Ren, M. Guo, X. Ye, J. Zhao, L. Xu, J. Qi, F. Kan, M. Liu, and D. Li. 2013. Synergistic effects of interleukin-1β and interleukin-17A antibodies on collagen-induced arthritis mouse model. *Int. Immunopharmacol.* 15: 199–205.
17. van den Berg, W. B., and I. B. McInnes. 2013. Th17 cells and IL-17 a—focus on immunopathogenesis and immunotherapeutics. *Semin. Arthritis Rheum.* 43: 158–170.
18. Nakae, S., A. Nambu, K. Sudo, and Y. Iwakura. 2003. Suppression of immune induction of collagen-induced arthritis in IL-17-deficient mice. *J. Immunol.* 171: 6173–6177.
19. Codarri, L., G. Gyülvészi, V. Tosevski, L. Hesske, A. Fontana, L. Magnenat, T. Suter, and B. Becher. 2011. RORγt drives production of the cytokine GM-CSF in helper T cells, which is essential for the effector phase of autoimmune neuroinflammation. *Nat. Immunol.* 12: 560–567.

20. El-Behi, M., B. Ciric, H. Dai, Y. Yan, M. Cullimore, F. Safavi, G. X. Zhang, B. N. Dittel, and A. Rostami. 2011. The encephalitogenicity of T(H)17 cells is dependent on IL-1- and IL-23-induced production of the cytokine GM-CSF. *Nat. Immunol.* 12: 568–575.
21. Ye, P., W. Chen, J. Wu, X. Huang, J. Li, S. Wang, Z. Liu, G. Wang, X. Yang, P. Zhang, et al. 2013. GM-CSF contributes to aortic aneurysms resulting from SMAD3 deficiency. *J. Clin. Invest.* 123: 2317–2331.
22. Wakasa-Morimoto, C., T. Toyosaki-Maeda, T. Matsutani, R. Yoshida, S. Nakamura-Kikuoka, M. Maeda-Tanimura, H. Yoshitomi, K. Hirota, M. Hashimoto, H. Masaki, et al. 2008. Arthritis and pneumonitis produced by the same T cell clones from mice with spontaneous autoimmune arthritis. *Int. Immunol.* 20: 1331–1342.
23. Nishikomori, R., R. O. Ehrhardt, and W. Strober. 2000. T helper type 2 cell differentiation occurs in the presence of interleukin 12 receptor beta2 chain expression and signaling. *J. Exp. Med.* 191: 847–858.
24. Frankel, S. K., B. M. Moats-Staats, C. D. Cool, M. W. Wynes, A. D. Stiles, and D. W. Riches. 2005. Human insulin-like growth factor-IA expression in transgenic mice promotes adenomatous hyperplasia but not pulmonary fibrosis. *Am. J. Physiol. Lung Cell. Mol. Physiol.* 288: L805–L812.
25. Yoshida, H., M. Hashizume, M. Suzuki, and M. Mihara. 2011. Induction of high-dose tolerance to the rat anti-mouse IL-6 receptor antibody in NZB/NZW F1 mice. *Rheumatol. Int.* 31: 1445–1449.
26. Tansey, D., A. U. Wells, T. V. Colby, S. Ip, A. Nikolakoupolou, R. M. du Bois, D. M. Hansell, and A. G. Nicholson. 2004. Variations in histological patterns of interstitial pneumonia between connective tissue disorders and their relationship to prognosis. *Histopathology* 44: 585–596.
27. de Lauretis, A., S. Veeraraghavan, and E. Renzoni. 2011. Review series: aspects of interstitial lung disease: connective tissue disease-associated interstitial lung disease: how does it differ from IPF? How should the clinical approach differ? *Chron. Respir. Dis.* 8: 53–82.
28. Bondeson, J., K. A. Browne, F. M. Brennan, B. M. Foxwell, and M. Feldmann. 1999. Selective regulation of cytokine induction by adenoviral gene transfer of IkappaBalpha into human macrophages: lipopolysaccharide-induced, but not zymosan-induced, proinflammatory cytokines are inhibited, but IL-10 is nuclear factor-kappaB independent. *J. Immunol.* 162: 2939–2945.
29. Lukens, J. R., M. J. Barr, D. D. Chaplin, H. Chi, and T. D. Kanneganti. 2012. Inflammasome-derived IL-1β regulates the production of GM-CSF by CD4(+) T cells and γδ T cells. *J. Immunol.* 188: 3107–3115.
30. Atamas, S. P., V. V. Yurovsky, R. Wise, F. M. Wigley, C. J. Goter Robinson, P. Henry, W. J. Alms, and B. White. 1999. Production of type 2 cytokines by CD8+ lung cells is associated with greater decline in pulmonary function in patients with systemic sclerosis. *Arthritis Rheum.* 42: 1168–1178.
31. Luzina, I. G., S. P. Atamas, R. Wise, F. M. Wigley, J. Choi, H. Q. Xiao, and B. White. 2003. Occurrence of an activated, profibrotic pattern of gene expression in lung CD8+ T cells from scleroderma patients. *Arthritis Rheum.* 48: 2262–2274.
32. Luzina, I. G., N. W. Todd, A. T. Iacono, and S. P. Atamas. 2008. Roles of T lymphocytes in pulmonary fibrosis. *J. Leukoc. Biol.* 83: 237–244.
33. Lo Re, S., D. Lison, and F. Huaux. 2013. CD4+ T lymphocytes in lung fibrosis: diverse subsets, diverse functions. *J. Leukoc. Biol.* 93: 499–510.
34. Vij, R., and M. E. Strek. 2013. Diagnosis and treatment of connective tissue disease-associated interstitial lung disease. *Chest* 143: 814–824.
35. Shimizu, Y., H. Kuwabara, A. Ono, S. Higuchi, T. Hisada, K. Dobashi, M. Utsugi, Y. Mita, and M. Mori. 2006. Intracellular Th1/Th2 balance of pulmonary CD4(+) T cells in patients with active interstitial pneumonia evaluated by serum KL-6. *Immunopharmacol. Immunotoxicol.* 28: 295–304.
36. Kolarz, G., O. Scherak, W. Popp, L. Ritschka, N. Thumb, A. Wottawa, and H. Zwick. 1993. Bronchoalveolar lavage in rheumatoid arthritis. *Br. J. Rheumatol.* 32: 556–561.
37. Nagasawa, Y., T. Takada, T. Shimizu, J. Narita, H. Moriyama, M. Terada, E. Suzuki, and F. Gejyo. 2009. Inflammatory cells in lung disease associated with rheumatoid arthritis. *Intern. Med.* 48: 1209–1217.
38. Enomoto, K., T. Takada, E. Suzuki, T. Ishida, H. Moriyama, H. Ooi, T. Hasegawa, H. Tsukada, M. Nakano, and F. Gejyo. 2003. Bronchoalveolar lavage fluid cells in mixed connective tissue disease. *Respirology* 8: 149–156.
39. Sauty, A., T. Rochat, O. D. Schoch, J. Hamacher, A. M. Kurt, J. M. Dayer, and L. P. Nicod. 1997. Pulmonary fibrosis with predominant CD8 lymphocytic alveolitis and anti-Jo-1 antibodies. *Eur. Respir. J.* 10: 2907–2912.
40. Yamadori, I., J. Fujita, H. Kajitani, S. Bandoh, M. Tokuda, Y. Yang, Y. Ohtsuki, T. Yoshinouchi, T. Kamei, and T. Ishida. 2000. Lymphocyte subsets in lung tissues of non-specific interstitial pneumonia and pulmonary fibrosis associated with collagen vascular disorders: correlation with CD4/CD8 ratio in bronchoalveolar lavage. *Lung* 178: 361–370.
41. Parajuli, B., Y. Sonobe, J. Kawanokuchi, Y. Doi, M. Noda, H. Takeuchi, T. Mizuno, and A. Suzumura. 2012. GM-CSF increases LPS-induced production of proinflammatory mediators via upregulation of TLR4 and CD14 in murine microglia. *J. Neuroinflammation* 9: 268.
42. Sorgi, C. A., S. Rose, N. Court, D. Carlos, F. W. Paula-Silva, P. A. Assis, F. G. Frantz, B. Ryffel, V. Quesniaux, and L. H. Faccioli. 2012. GM-CSF priming drives bone marrow-derived macrophages to a pro-inflammatory pattern and downmodulates PGE2 in response to TLR2 ligands. *PLoS One* 7: e40523.
43. Berclaz, P. Y., B. Carey, M. D. Fillipi, K. Wernke-Dollries, N. Geraci, S. Cush, T. Richardson, J. Kitzmiller, M. O'Connor, C. Hermoyian, et al. 2007. GM-CSF regulates a PU.1-dependent transcriptional program determining the pulmonary response to LPS. *Am. J. Respir. Cell Mol. Biol.* 36: 114–121.
44. Sonderegger, I., G. Iezzi, R. Maier, N. Schmitz, M. Kurrer, and M. Kopf. 2008. GM-CSF mediates autoimmunity by enhancing IL-6-dependent Th17 cell development and survival. *J. Exp. Med.* 205: 2281–2294.
45. Khameneh, H. J., S. A. Isa, L. Min, F. W. Nih, and C. Ruedl. 2011. GM-CSF signalling boosts dramatically IL-1 production. *PLoS One* 6: e23025.
46. Shi, Y., C. H. Liu, A. I. Roberts, J. Das, G. Xu, G. Ren, Y. Zhang, L. Zhang, Z. R. Yuan, H. S. Tan, et al. 2006. Granulocyte-macrophage colony-stimulating factor (GM-CSF) and T-cell responses: what we do and don't know. *Cell Res.* 16: 126–133.
47. Johnson, G. R., T. J. Gonda, D. Metcalf, I. K. Hariharan, and S. Cory. 1989. A lethal myeloproliferative syndrome in mice transplanted with bone marrow cells infected with a retrovirus expressing granulocyte-macrophage colony stimulating factor. *EMBO J.* 8: 441–448.
48. Kolls, J. K., and A. Lindén. 2004. Interleukin-17 family members and inflammation. *Immunity* 21: 467–476.
49. Tang, H., S. Pang, M. Wang, X. Xiao, Y. Rong, H. Wang, and Y. Q. Zang. 2010. TLR4 activation is required for IL-17-induced multiple tissue inflammation and wasting in mice. *J. Immunol.* 185: 2563–2569.
50. Spurlock, N. K., and J. E. Prittie. 2011. A review of current indications, adverse effects, and administration recommendations for intravenous immunoglobulin. *J. Vet. Emerg. Crit. Care* 21: 471–483.
51. Greenhill, S. R., and D. N. Kotton. 2009. Pulmonary alveolar proteinosis: a bench-to-bedside story of granulocyte-macrophage colony-stimulating factor dysfunction. *Chest* 136: 571–577.
52. Dranoff, G., A. D. Crawford, M. Sadelain, B. Ream, A. Rashid, R. T. Bronson, G. R. Dickersin, C. J. Bachurski, E. L. Mark, J. A. Whitsett, et al. 1994. Involvement of granulocyte-macrophage colony-stimulating factor in pulmonary homeostasis. *Science* 264: 713–716.
53. Vlahos, R., S. Bozinovski, J. A. Hamilton, and G. P. Anderson. 2006. Therapeutic potential of treating chronic obstructive pulmonary disease (COPD) by neutralising granulocyte macrophage-colony stimulating factor (GM-CSF). *Pharmacol. Ther.* 112: 106–115.
54. Burmester, G. R., M. E. Weinblatt, I. B. McInnes, D. Porter, O. Barbarash, M. Vatutin, I. Szombati, E. Esfandiari, M. A. Sleeman, and C. D. Kane, et al. 2013. Efficacy and safety of mavrilimumab in subjects with rheumatoid arthritis. *Ann. Rheum. Dis.* 72: 1445-1452.

ARTHRITIS & RHEUMATOLOGY
Vol. 66, No. 7, July 2014, pp 1864–1871
DOI 10.1002/art.38630

A Crucial Role of L-Selectin in C Protein–Induced Experimental Polymyositis in Mice

Kyosuke Oishi,[1] Yasuhito Hamaguchi,[1] Takashi Matsushita,[1] Minoru Hasegawa,[1] Naoko Okiyama,[2] Jens Dernedde,[3] Marie Weinhart,[4] Rainer Haag,[4] Thomas F. Tedder,[5] Kazuhiko Takehara,[1] Hitoshi Kohsaka,[2] and Manabu Fujimoto[1]

Objective. **To investigate the role of adhesion molecules in C protein–induced myositis (CIM), a murine model of polymyositis (PM).**

Methods. **CIM was induced in wild-type mice, L-selectin–deficient (L-selectin$^{-/-}$) mice, intercellular adhesion molecule 1 (ICAM-1)–deficient (ICAM-1$^{-/-}$) mice, and mice deficient in both L-selectin and ICAM-1 (L-selectin$^{-/-}$ICAM-1$^{-/-}$ mice). Myositis severity, inflammatory cell infiltration, and messenger RNA expression in the inflamed muscles were analyzed. The effect of dendritic polyglycerol sulfate, a synthetic inhibitor that suppresses the function of L-selectin and endothelial P-selectin, was also examined.**

Results. **L-selectin$^{-/-}$ mice and L-selectin$^{-/-}$ ICAM-1$^{-/-}$ mice developed significantly less severe myositis compared to wild-type mice, while ICAM-1 deficiency did not inhibit the development of myositis. L-selectin$^{-/-}$ mice that received wild-type T cells developed myositis. Treatment with dendritic polyglycerol sulfate significantly diminished the severity of myositis in wild-type mice compared to treatment with control.**

Conclusion. **These data indicate that L-selectin plays a major role in the development of CIM, whereas ICAM-1 plays a lesser role, if any, in the development of CIM. L-selectin–targeted therapy may be a candidate for the treatment of PM.**

Polymyositis (PM) is a chronic autoimmune inflammatory myopathy. It affects striated muscles and induces varying degrees of weakness, especially in the proximal muscles (1). Although the pathogenesis of PM has not been elucidated, cytotoxic CD8+ T cells are thought to play a prominent role in the development of myositis (2). Recently, the C protein–induced myositis (CIM) model was established as an animal model of PM (3). The skeletal muscle C protein is a myosin-binding protein that regulates muscle filament components (4). This murine myositis is readily induced by a single immunization with recombinant skeletal muscle C protein fragments in C57BL/6 mice. CIM elicits abundant perforin-positive CD8+ T cells that infiltrate endomysial sites. In addition, CD8+ T cell depletion inhibits the progression of myositis. In the CIM model, inflammatory cytokines, including interleukin-1 (IL-1), IL-6, and tumor necrosis factor α (TNFα), mediate the induction and development of myositis (3,5,6). The CIM model is primarily used to examine the inflammatory phase of PM.

Leukocyte recruitment into sites of inflammation is accomplished by constitutive or inducible expression of multiple adhesion molecules (7–9). L-selectin (CD62L), which primarily mediates leukocyte capture and rolling on the endothelium, is constitutively expressed by most leukocytes (10). In addition, L-selectin plays significant roles in the activation of multiple intracellular signaling pathways (11). Intercellular adhesion

Supported by the Ministry of Health, Labor, and Welfare of Japan and the Ministry of Education, Culture, Sports, Science, and Technology of Japan (intractable diseases research grant), the DFG (grant to the Collaborative Research Center SFB 765), and the NIH (grant AI-056363 to Dr. Tedder).

[1]Kyosuke Oishi, MD, Yasuhito Hamaguchi, MD, PhD, Takashi Matsushita, MD, PhD, Minoru Hasegawa, MD, PhD, Kazuhiko Takehara, MD, PhD, Manabu Fujimoto, MD: Kanazawa University, Kanazawa, Japan; [2]Naoko Okiyama, MD, PhD, Hitoshi Kohsaka, MD, PhD: Tokyo Medical and Dental University, Tokyo, Japan; [3]Jens Dernedde, PhD: Charité–Universitätsmedizin Berlin, Berlin, Germany; [4]Marie Weinhart, PhD, Rainer Haag, PhD: Freie Universität, Berlin, Germany; [5]Thomas F. Tedder, PhD: Duke University Medical Center, Durham, North Carolina.

Address correspondence to Yasuhito Hamaguchi, MD, PhD, Department of Dermatology, Faculty of Medicine, Institute of Medical, Pharmaceutical, and Health Sciences, Kanazawa University, 13-1 Takaramachi, Kanazawa, Ishikawa 920-8641, Japan. E-mail: yasuhito@med.kanazawa-u.ac.jp.

Submitted for publication July 16, 2013; accepted in revised form March 11, 2014.

molecule 1 (ICAM-1; CD54) is a member of the Ig superfamily that is constitutively expressed on endothelial cells, subsets of leukocytes, fibroblasts, and epithelial cells (12). It can be transcriptionally up-regulated by several proinflammatory cytokines, such as TNFα, interferon-γ (IFNγ), and IL-1 (12). L-selectin and ICAM-1 act in concert with each other during leukocyte migration from blood to extravascular tissues where inflammatory responses occur in vivo (13,14).

The relative contributions of L-selectin and ICAM-1 are largely dependent on the type of model of inflammation being used. For instance, in the immediate-type hypersensitivity model, deficiency of either L-selectin or ICAM-1 resulted in the immune response being reduced to similar degrees. Deficiency of both L-selectin and ICAM-1 did not exhibit a synergistic effect (15). Introducing defective ICAM-1 into L-selectin–deficient (L-selectin$^{-/-}$) mice resulted in a profoundly decreased pulmonary fibrosis compared to that observed in mice with a deficiency of a single adhesion molecule in a bleomycin-induced pulmonary fibrosis model (16). However, wound healing was not inhibited by L-selectin deficiency, while delayed wound healing was observed in ICAM-1-deficient (ICAM-1$^{-/-}$) mice (17). Nevertheless, the relative contributions and interaction of L-selectin and ICAM-1 in the CIM model remain unknown.

In this study, we investigated the role of adhesion molecules in CIM by using L-selectin$^{-/-}$ mice, ICAM-1$^{-/-}$ mice, and L-selectin and ICAM-1 double-deficient (L-selectin$^{-/-}$ICAM-1$^{-/-}$) mice. Inhibition of L-selectin ameliorated the severity of myositis. The results of this study indicate that L-selectin contributes to the development of CIM more than ICAM-1 does, and that L-selectin might serve as a therapeutic target for the treatment of PM.

MATERIALS AND METHODS

Mice. L-selectin$^{-/-}$ mice were produced as previously described (18). ICAM-1$^{-/-}$ mice (19) were from The Jackson Laboratory, and L-selectin$^{-/-}$ICAM-1$^{-/-}$ mice were generated as previously described (14). All mice were backcrossed more than 8 generations onto the C57BL/6 genetic background. Female mice ages 8–10 weeks were used in the experiments. Age-matched C57BL/6 mice (The Jackson Laboratory) were used as controls. All mice were housed in a specific pathogen–free barrier facility and screened regularly for pathogens. The Committee on Animal Experimentation of Kanazawa University Graduate School of Medical Science approved all studies and procedures.

CIM induction. To induce CIM, 8–10-week-old female mice were immunized intradermally with 200 μg of murine C protein fragments (3) emulsified in 200 μl of Freund's complete adjuvant (CFA) containing 100 μg of heat-killed *Mycobacterium butyricum* (Difco) (5). The immunogens were injected at multiple sites in the back and footpads. Pertussis toxin (0.2–2 μg; Seikagaku) in phosphate buffered saline (PBS) was injected intraperitoneally at the same time.

Mice were killed on day 14 after immunization with C protein, and muscle tissue specimens were harvested. Hematoxylin and eosin (H&E)–stained 10-μm sections of the hamstrings and quadriceps were examined histologically. The histologic severity of myositis in each muscle block was graded (3) on a scale of 1–4, where 1 = involvement of $\geq$1 muscle fiber but <5 muscle fibers, 2 = a lesion involving 5–30 muscle fibers, 3 = a lesion involving a muscle fasciculus, and 4 = diffuse, extensive lesions. When multiple lesions with the same grade were found in a single muscle block, 0.5 was added to the grade. We also assessed necrotic muscle areas. Necrotic muscle areas were quantified by measuring necrotic muscle fibers showing decreased H&E staining and the replacement of muscle fibers by mononuclear cell infiltrates (6).

Immunohistochemical staining. Muscle sections (4 μm thick) obtained from the left thighs of the mice were frozen in cold 2-methylbutane and were stained with anti-CD8a (53-6.7) and anti-CD4 (RM4-5) (BD Biosciences). Muscle sections (4 μm thick) obtained from the right thighs of the mice were fixed in formalin, dehydrated, embedded in paraffin, and then incubated with rat monoclonal antibodies specific for CD3 (CD3-12; Serotec), F4/80 (A3-1; Abcam), and myeloperoxidase (MPO; NeoMarkers). Six inflammatory mononuclear cell foci in the serial sections were studied. Stained cells were counted in every focus under high magnification (400×) using a light microscope. The mean score was used for analysis. The stained sections were evaluated by 2 independent observers who reported comparable results.

Adoptive transfer of mouse spleen T cells. Single-cell suspensions of splenic leukocytes from naive, nonimmunized wild-type mice were generated by gentle homogenization. CD90.2 monoclonal antibody–coupled microbeads were used to purify T cell populations according to the recommendations of the manufacturer (Miltenyi Biotech). The purity of extracted T cells from donor mice was measured using a FACSCanto II flow cytometer (BD Biosciences), and purities were >90%. Viable spleen T cells (8×10^6) were transferred intravenously into recipient L-selectin$^{-/-}$ mice. Twenty-four hours after adoptive transfer of T cells, recipient L-selectin$^{-/-}$ mice were immunized with C protein fragments, and 14 days after immunization their muscles were harvested as described above. PBS-injected mice were used as controls.

Real-time reverse transcription–polymerase chain reaction (RT-PCR). Total RNAs were extracted from muscle samples using Qiagen RNeasy spin columns, and real-time RT-PCR was performed using a TaqMan system (Applied Biosystems) on an ABI Prism 7000 Sequence Detector (Applied Biosystems) (20). TaqMan probes and primers for IL-1β, IL-6, IL-10, IL-12α, IFNγ, TNFα, monocyte chemoattractant protein 1 (MCP-1), and GAPDH were purchased from Applied Biosystems. Relative expression of RT-PCR products was determined using the $\Delta\Delta C_t$ technique. Each reaction was performed at least in triplicate.

Treatment of mice with dendritic polyglycerol sulfate. Dendritic polyglycerol sulfates are multivalent inhibitors of

inflammation that inhibit both L-selectin and endothelial P-selectin with high efficacy (21). Wild-type mice were injected subcutaneously with dendritic polyglycerol sulfate (0.3 mg/mouse) into the shaved neck for 11 consecutive days, beginning 3 days after immunization with C protein. Mice injected subcutaneously with PBS were used as controls.

Statistical analysis. The Mann-Whitney U test was used to determine the level of significance of differences in the sample means. The Bonferroni test was used for multiple comparisons. All statistical analysis was performed using Prism software.

RESULTS

Amelioration of myositis severity in L-selectin–deficient mice. To determine if adhesion molecules play a role in myositis, we assessed the severity of myositis in wild-type, L-selectin$^{-/-}$, ICAM-1$^{-/-}$, and L-selectin$^{-/-}$ ICAM-1$^{-/-}$ mice (Figure 1A). Histologic scores were significantly lower in L-selectin$^{-/-}$ mice than in wild-type mice ($P < 0.01$) (Figure 1B). Similarly, ICAM-1$^{-/-}$ mice demonstrated a 50% decrease in myositis severity score compared to wild-type mice, although the differences did not reach significance. L-selectin$^{-/-}$ ICAM-1$^{-/-}$ mice displayed significantly lower histologic scores compared to wild-type mice ($P < 0.01$). Histologic scores in L-selectin$^{-/-}$ and L-selectin$^{-/-}$ ICAM-1$^{-/-}$ mice were also significantly lower than those in ICAM-1$^{-/-}$ mice ($P < 0.01$ for both).

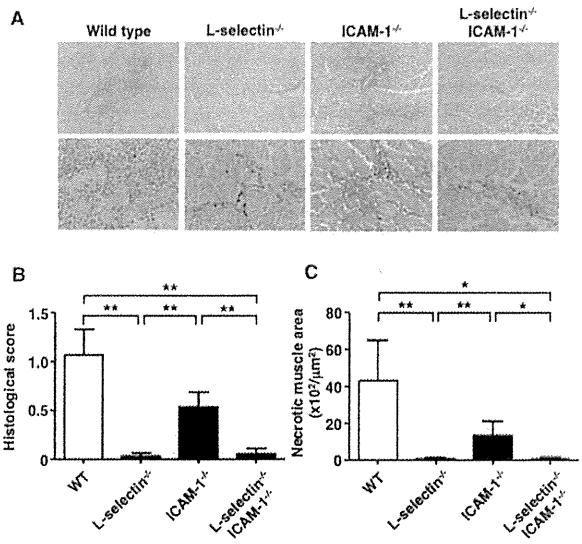

Figure 1. C protein–induced myositis in wild-type (WT) mice, L-selectin–deficient mice, ICAM-1–deficient mice, and mice deficient in both L-selectin and ICAM-1. Mice were killed on day 14 after immunization with C protein, and muscle tissue specimens were harvested. **A,** Representative images of muscle inflammation in the indicated mouse genotypes. Hematoxylin and eosin stained. Original magnification × 100 in top panels; × 400 in bottom panels. **B** and **C,** Histologic score (**B**) and area of muscle fiber necrosis (**C**) in each mouse group. Bars show the mean ± SEM (n = 8–10 mice per genotype). * = $P < 0.05$; ** = $P < 0.01$.

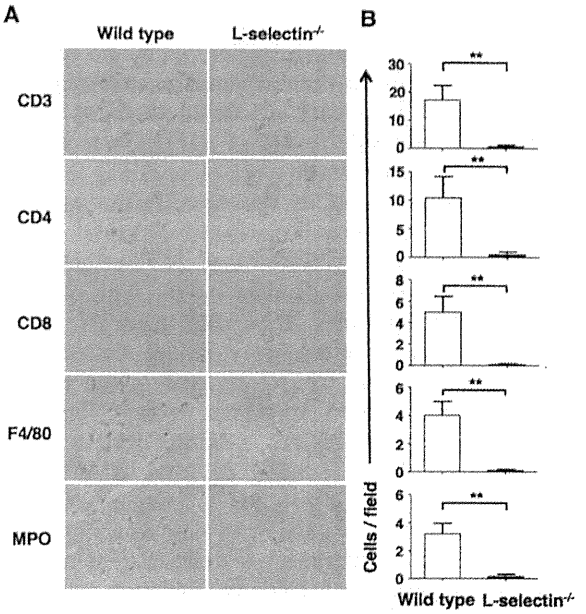

Figure 2. Inflammatory cell infiltration into the inflamed muscles of wild-type and L-selectin$^{-/-}$ mice with C protein–induced myositis. Mice were killed on day 14 after immunization with C protein, and muscle tissue specimens were harvested. **A,** Representative immunohistochemical images showing CD3, CD4, CD8, F4/80, and myeloperoxidase (MPO) staining in tissue sections from wild-type and L-selectin$^{-/-}$ mice. Original magnification × 400. **B,** Numbers of CD3+, CD4+, and CD8+ T cells, F4/80-positive macrophages, and MPO-positive neutrophils in wild-type and L-selectin$^{-/-}$ mice on day 14. Bars show the mean ± SEM (n = 8–10 mice per genotype). ** = $P < 0.01$.

We also assessed necrotic muscle areas to evaluate muscle damage in the mice (Figure 1C). Necrotic muscle areas were significantly smaller in L-selectin$^{-/-}$ mice than in wild-type mice ($P < 0.01$). ICAM-1$^{-/-}$ mice showed a 69% decrease in necrotic muscle areas compared to wild-type mice. L-selectin$^{-/-}$ICAM-1$^{-/-}$ mice displayed significantly decreased necrotic muscle areas comparable to those of L-selectin$^{-/-}$ mice. Necrotic muscle areas in L-selectin$^{-/-}$ and L-selectin$^{-/-}$ ICAM-1$^{-/-}$ mice were also significantly smaller than those in ICAM-1$^{-/-}$ mice ($P < 0.01$ and $P < 0.05$, respectively). Histologic scores paralleled the increases in necrotic muscle areas. L-selectin$^{-/-}$ and L-selectin$^{-/-}$

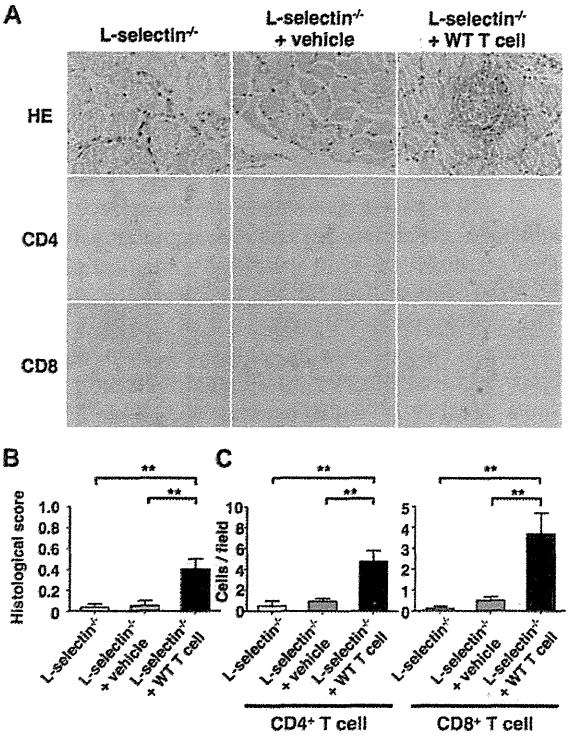

Figure 3. Adoptive transfer of T cells from wild-type (WT) mice into L-selectin$^{-/-}$ mice. Mice were killed on day 14 after immunization with C protein, and muscle tissue specimens were harvested. **A,** Representative muscle sections stained with hematoxylin and eosin (H&E) and immunohistochemical images showing CD4 and CD8 staining in sections from L-selectin$^{-/-}$ mice, L-selectin$^{-/-}$ mice treated with vehicle, and L-selectin$^{-/-}$ mice that received wild-type T cells. Original magnification × 400. **B,** Histologic score in each mouse group. **C,** Numbers of CD4+ and CD8+ T cells. Bars in **B** and **C** show the mean ± SEM (n = 5 mice per group). ** = $P < 0.01$.

ICAM-1$^{-/-}$ mice developed a minimal degree of myositis. These results suggest that L-selectin contributes profoundly to the development of CIM, whereas the contribution of ICAM-1 is less relevant.

Reduced leukocyte recruitment in L-selectin–deficient mice. Since L-selectin$^{-/-}$ mice, but not ICAM-1$^{-/-}$ mice, showed significantly less severe myositis compared to wild-type mice, we assessed inflammatory cell infiltration in the inflamed muscles of wild-type mice and L-selectin$^{-/-}$ mice (Figures 2A and B). Immunohistologic staining revealed that CD3+, CD4+, and CD8+ T cells, F4/80-positive macrophages, and MPO-positive neutrophils were all significantly reduced in L-selectin$^{-/-}$ mice compared to wild-type mice ($P <$ 0.01 for all comparisons). We detected very few B220+ B cells in the inflamed muscles of either wild-type mice or L-selectin$^{-/-}$ mice (data not shown). These results suggest that L-selectin plays an important role in the migration of leukocytes into inflamed muscles in the CIM model.

Development of myositis in L-selectin$^{-/-}$ mice that received wild-type T cells. Although L-selectin is expressed on various leukocyte subsets, CD8+ T cells are considered to be crucial for the induction of CIM. Therefore, we performed adoptive transfer experiments to confirm the importance of L-selectin expression on T cells. As described above, L-selectin$^{-/-}$ mice exhibited minimal development of myositis. In contrast, L-selectin$^{-/-}$ mice that received T cells from naive, nonimmunized wild-type mice developed readily apparent myositis. Histologic scores in L-selectin$^{-/-}$ mice that received wild-type T cells were ~10-fold higher than those of L-selectin$^{-/-}$ mice and L-selectin$^{-/-}$ mice treated with vehicle ($P < 0.01$ for both) (Figures 3A and B). Although the histologic scores in L-selectin$^{-/-}$ mice that received wild-type T cells were 52% lower than those in wild-type mice, the difference did not reach significance. Our analysis of cell infiltration showed that both CD4+ and CD8+ T cells were more abundant in L-selectin$^{-/-}$ mice that received wild-type T cells (Figure 3C). These results indicate that L-selectin expression on T cells is important for leukocyte migration into inflamed muscles and the development of myositis in mice.

Cytokine expression in CIM. We next compared messenger RNA (mRNA) expression in inflamed muscles from wild-type and L-selectin$^{-/-}$ mice by RT-PCR (Figure 4). The levels of mRNA for IL-6, IL-10, IL-12,

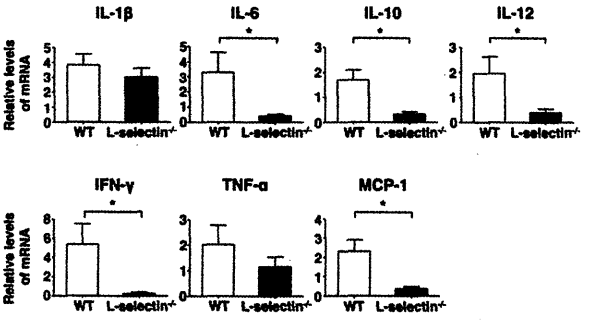

Figure 4. Levels of mRNA in the inflamed muscles from wild-type (WT) and L-selectin$^{-/-}$ mice on day 14 after immunization with C protein. Bars show the mean ± SEM (n = 5 or more mice per genotype). * = $P < 0.05$. IL-1β = interleukin-1β; IFNγ = interferon-γ; TNFα = tumor necrosis factor α; MCP-1 = monocyte chemoattractant protein 1.

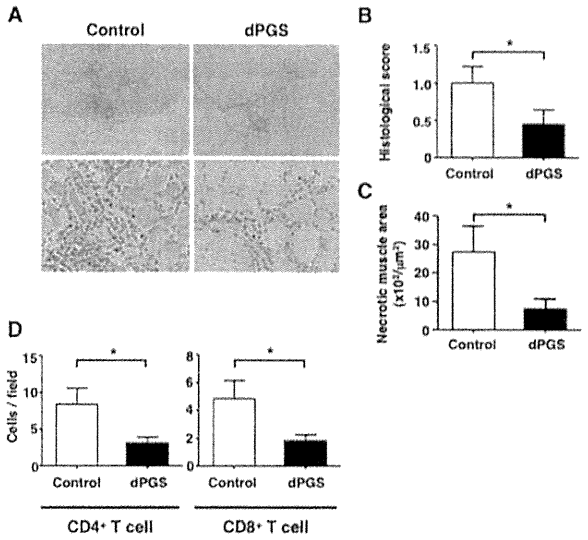

Figure 5. Decreased severity of myositis in wild-type mice treated with dendritic polyglycerol sulfate (dPGS). Dendritic polyglycerol sulfate was injected into mice intradermally for 11 consecutive days, beginning 3 days after immunization with C protein. Mice were killed on day 14 after immunization, and muscle tissue specimens were harvested. **A**, Representative images of muscle inflammation in wild-type mice treated with dendritic polyglycerol sulfate or phosphate buffered saline (control). Hematoxylin and eosin stained. Original magnification × 100 in top panels; × 400 in bottom panels. **B** and **C**, Histologic scores (**B**) and area of muscle fiber necrosis (**C**) in each mouse group. **D**, Numbers of CD4+ and CD8+ T cells on day 14. Bars in **B–D** show the mean ± SEM (n = 8–10 mice per group). * = $P < 0.05$.

IFNγ, and MCP-1 were significantly reduced in L-selectin$^{-/-}$ mice compared to wild-type mice ($P < 0.05$ for all comparisons). IL-1β and TNFα mRNA expression levels in L-selectin$^{-/-}$ mice were decreased 21% and 43%, respectively, compared to wild-type mice, but the differences did not reach significance for either cytokine.

Diminished severity of myositis in mice treated with dendritic polyglycerol sulfate. Since dendritic polyglycerol sulfate is an inhibitor that suppresses the function of adhesion molecules, including L-selectin, wild-type mice were treated with dendritic polyglycerol sulfate. Wild-type mice treated with dendritic polyglycerol sulfate showed 52% lower histologic scores than PBS-treated control wild-type mice ($P < 0.05$) (Figures 5A and B). Necrotic tissue areas from wild-type mice treated with dendritic polyglycerol sulfate were significantly smaller than those from PBS-treated control wild-type mice ($P < 0.05$) (Figure 5C). Infiltration of both CD4+ and CD8+ T cells was also significantly decreased by dendritic polyglycerol sulfate treatment (Figure 5D).

DISCUSSION

This is the first study to reveal the roles of adhesion molecules in the development of CIM, a murine model of PM. Specifically, L-selectin, but not ICAM-1, was critical for the development of myositis. The development of myositis was also prevented by treatment with dendritic polyglycerol sulfate, which binds to L-selectin and endothelial P-selectin and prevents leukocytes from binding to inflamed vascular endothelia (21). Thus, our findings indicate that L-selectin plays a critical role in the development of CIM, and that L-selectin could be a target for the treatment of PM.

The cell adhesion molecules L-selectin and ICAM-1 act cooperatively to mediate optimal leukocyte rolling and the recruitment of leukocytes to sites of inflammation (13,14,22–24). Although the relative contributions of L-selectin and ICAM-1 vary among different models of inflammation, ICAM-1 appears to play a more predominant role than L-selectin in general. However, this study indicates that L-selectin is more important than ICAM-1 in the development of CIM (Figures 1A and B).

Previous studies clearly indicate that CD8+ T cells play a more significant role than CD4+ T cells in the development of CIM. Tang et al (25) reported that the percentage of L-selectin–positive cells in CD8+ T cells was greater than that in CD4+ T cells, especially in lymphoid tissues, and that L-selectin expression levels were higher on CD8+ T cells than on CD4+ T cells in wild-type mice. In contrast, L-selectin deficiency did not affect ICAM-1 expression (16). Thus, the different expression levels of L-selectin between CD4+ and CD8+ T cells may partly explain the finding that L-selectin deficiency had a greater effect on the degree of myositis than ICAM-1 did in the present study. Alternatively, the greater role of L-selectin may be explained by the fact that L-selectin is important for antiviral immunity (26) and antitumor activity (27), in which CD8+ cytotoxic T cells play a substantial role. The etiologic role of CD8+ cytotoxic T cells may be another reason why L-selectin is more important than ICAM-1 in the CIM model.

It is assumed that leukocyte infiltration and cytokines participate in the development of CIM. Consistent with this, L-selectin$^{-/-}$ mice exhibited significantly decreased numbers of leukocytes, including CD4+ and

CD8+ T cells, F4/80-positive macrophages, and MPO-positive neutrophils, in the inflamed muscles on day 14 following CIM induction (Figures 2A and B). In addition, adoptive transfer of wild-type T cells induced myositis in L-selectin$^{-/-}$ mice (Figures 3A–C). These data suggest that L-selectin expression on T cells is required for the induction of myositis via the recruitment of leukocytes into the muscles. However, alternatives should be considered to explain the reduction in myositis severity seen in L-selectin$^{-/-}$ mice. It has been reported that myositis development required both the activation of T cells and the conditioning of local muscle tissue as a "seed and soil" model, and CIM regression was due to attenuation of local CFA-induced immune activation (28). Thus, local immune activation in L-selectin$^{-/-}$ mice might be impaired, leading to reduced myositis severity.

L-selectin expression on leukocytes may be important not only for leukocyte infiltration, but also for subsequent cytokine production. In the CIM model, IL-6 deficiency inhibited the progression of myositis, and IL-6 blockade reduced the severity of myositis (5). Consistent with this previous report, our study showed that IL-6 mRNA expression in the inflamed muscles of L-selectin$^{-/-}$ mice was significantly decreased compared to that in wild-type mice (Figure 4). Moreover, other inflammatory cytokines, including IL-12 and IFNγ, were decreased in L-selectin$^{-/-}$ mice as well. The incidence of myositis in IL-1–deficient and TNFα-deficient mice was significantly lower than that in wild-type mice (3). Although the differences did not reach significance, IL-1β and TNFα tended to decrease in L-selectin$^{-/-}$ mice compared to wild-type mice in this study (Figure 4). Taken together, these findings indicate that L-selectin expression influences cytokine production in inflamed mouse muscles. However, the mechanism by which L-selectin is involved in cytokine regulation needs to be evaluated.

The establishment of effective PM therapies has long been awaited. Corticosteroids have been proven to be beneficial, but serious adverse effects can frequently occur. To date, several studies targeting adhesion molecules have been performed. Bimosiamose is a small-molecule and pan-selectin antagonist that targets E-selectin, P-selectin, and L-selectin (29). Inhaled administration of bimosiamose in asthmatic patients was shown to attenuate late asthmatic reactions (30). Subcutaneous administration of bimosiamose improved the clinical scores in patients with psoriasis (31). A humanized anti–L-selectin monoclonal antibody (aselizumab) significantly increased survival time and decreased mortality in a baboon model of hemorrhagic-traumatic shock (32). However, intravenous administration of aselizumab to multiple traumatized patients resulted in no significant improvement of efficacy in a phase II clinical trial (33). Also, caution should be paid in developing biologic therapies targeting adhesion molecules. A humanized anti-CD11a monoclonal antibody, efalizumab, was effective for the treatment of psoriasis, but a long-term followup study revealed several fatal cases of progressive multifocal leukoencephalopathy by JC virus (34), leading to voluntary withdrawal of the drug from the market. In this study, the synthetic compound dendritic polyglycerol sulfate, which is an inhibitor that suppresses the function of leukocytic L-selectin and endothelial P-selectin, improved myositis severity (Figures 5A–C). Therefore, we assume that a selectin-targeted therapy could still be an option for the treatment of PM.

We are well aware that our study is impacted by a number of limitations. First, the murine CIM model of PM that was used only mimics the inflammatory aspect of the human disease. Second, immune responses against C protein have not been reported in human PM patients. Third, we did not conduct functional assays to directly assess muscle weakness in this study. In previous experiments, we attempted several assays, including a rotarod performance test and the measurement of serum creatinine kinase. We used rotarod tests in a previous study (3). However, according to our experience, the rotarod test turned out to be less reliable than histologic analyses, because mice learn how to avoid falling off and do not necessarily run consistently. In addition, serum levels of creatinine kinase or other muscle-derived proteins are unreliable parameters. They are often high in normal mice, presumably because of their physical activity (28). Devices are needed to directly quantify rodent muscle strength to best observe the clinical course of the disease.

In conclusion, immune cell infiltration initiated via selectin–ligand interactions and the production of proinflammatory cytokines, such as IL-6, and chemoattractants for inflammatory cells, such as MCP-1, may be a trigger of myositis in CIM. Our findings also indicate that the cell adhesion molecule L-selectin may be a candidate for treating PM, an intractable autoimmune disease.

ACKNOWLEDGMENTS

We thank Ms E. Yoshimoto, Ms M. Matsubara, and Ms Y. Yamada for technical assistance.

AUTHOR CONTRIBUTIONS

All authors were involved in drafting the article or revising it critically for important intellectual content, and all authors approved the final version to be published. Dr. Hamaguchi had full access to all of the data in the study and takes responsibility for the integrity of the data and the accuracy of the data analysis.

Study conception and design. Oishi, Hamaguchi, Kohsaka, Fujimoto.
Acquisition of data. Oishi, Hamaguchi, Dernedde, Weinhart, Haag, Tedder, Kohsaka.
Analysis and interpretation of data. Oishi, Hamaguchi, Matsushita, Hasegawa, Okiyama, Takehara, Kohsaka, Fujimoto.

REFERENCES

1. Dalakas MC, Hohlfeld R. Polymyositis and dermatomyositis. Lancet 2003;362:971–82.
2. Engel AG, Arahata K, Emslie-Smith A. Immune effector mechanisms in inflammatory myopathies. Res Publ Assoc Res Nerv Ment Dis 1990;68:141–57.
3. Sugihara T, Sekine C, Nakae T, Kohyama K, Harigai M, Iwakura Y, et al. A new murine model to define the critical pathologic and therapeutic mediators of polymyositis. Arthritis Rheum 2007;56: 1304–14.
4. Gilbert R, Cohen JA, Pardo S, Basu A, Fischman DA. Identification of the A-band localization domain of myosin binding proteins C and H (MyBP-C, MyBP-H) in skeletal muscle. J Cell Sci 1999;112:69–79.
5. Okiyama N, Sugihara T, Iwakura Y, Yokozeki H, Miyasaka N, Kohsaka H. Therapeutic effects of interleukin-6 blockade in a murine model of polymyositis that does not require interleukin-17A. Arthritis Rheum 2009;60:2505–12.
6. Sugihara T, Okiyama N, Suzuki M, Kohyama K, Matsumoto Y, Miyasaka N, et al. Definitive engagement of cytotoxic CD8 T cells in C protein–induced myositis, a murine model of polymyositis. Arthritis Rheum 2010;62:3088–92.
7. Springer TA. Traffic signals for lymphocyte recirculation and leukocyte emigration: the multistep paradigm. Cell 1994;76: 301–14.
8. Ley K, Kansas GS. Selectins in T-cell recruitment to non-lymphoid tissues and sites of inflammation. Nat Rev Immunol 2004;4: 325–35.
9. Luster AD, Alon R, von Andrian UH. Immune cell migration in inflammation: present and future therapeutic targets. Nat Immunol 2005;6:1182–90.
10. Tedder TF, Steeber DA, Pizcueta P. L-selectin deficient mice have impaired leukocyte recruitment into inflammatory sites. J Exp Med 1995;181:2259–64.
11. Grailer JJ, Kodera M, Steeber DA. L-selectin: role in regulating homeostasis and cutaneous inflammation. J Dermatol Sci 2009;56: 141–7.
12. Dustin ML, Rothlein R, Bhan AK, Dinarello CA, Springer TA. Induction by IL 1 and interferon-γ: tissue distribution, biochemistry, and function of a natural adherence molecule (ICAM-1). J Immunol 1986;137:245–53.
13. Steeber DA, Tang ML, Green NE, Zhang XQ, Sloane JE, Tedder TF. Leukocyte entry into sites of inflammation requires overlapping interactions between the L-selectin and intercellular adhesion molecule-1 pathways. J Immunol 1999;163:2176–86.
14. Steeber DA, Campbell MA, Basit A, Ley K, Tedder TF. Optimal selectin-mediated rolling of leukocytes during inflammation in vivo requires intercellular adhesion molecule-1 expression. Proc Natl Acad Sci U S A 1998;95:7562–7.
15. Shimada Y, Hasegawa M, Kaburagi Y, Hamaguchi Y, Komura K, Saito E, et al. L-selectin or ICAM-1 deficiency reduces an immediate-type hypersensitivity response by preventing mast cell recruitment in repeated elicitation of contact hypersensitivity. J Immunol 2003;170:4325–34.
16. Hamaguchi Y, Nishizawa Y, Yasui M, Hasegawa M, Kaburagi Y, Komura K, et al. Intercellular adhesion molecule-1 and L-selectin regulate bleomycin-induced lung fibrosis. Am J Pathol 2002;161: 1607–18.
17. Nagaoka T, Kaburagi Y, Hamaguchi Y, Hasegawa M, Takehara K, Steeber DA, et al. Delayed wound healing in the absence of intercellular adhesion molecule-1 or L-selectin expression. Am J Pathol 2000;157:237–47.
18. Arbones ML, Ord DC, Ley K, Ratech H, Maynard-Curry C, Otten G, et al. Lymphocyte homing and leukocyte rolling and migration are impaired in L-selectin deficient mice. Immunity 1994;1: 247–60.
19. Sligh JE Jr, Ballantyne CM, Rich SS, Hawkins HK, Smith CW, Bradley A, et al. Inflammatory and immune responses are impaired in mice deficient in intercellular adhesion molecule 1. Proc Natl Acad Sci U S A 1993;90:8529–33.
20. Maeda S, Fujimoto M, Matsushita T, Hamaguchi Y, Takehara K, Hasegawa M. Inducible costimulator (ICOS) and ICOS ligand signaling has pivotal roles in skin wound healing via cytokine production. Am J Pathol 2011;179:2360–9.
21. Dernedde J, Rausch A, Weinhart M, Enders S, Tauber R, Licha K, et al. Dendritic polyglycerol sulfates as multivalent inhibitors of inflammation. Proc Natl Acad Sci U S A 2010;107:19679–84.
22. Kaburagi Y, Hasegawa M, Nagaoka T, Shimada Y, Hamaguchi Y, Komura K, et al. The cutaneous reverse Arthus reaction requires intercellular adhesion molecule 1 and L-selectin expression. J Immunol 2002;168:2970–8.
23. Komura K, Hasegawa M, Hamaguchi Y, Saito E, Kaburagi Y, Yanaba K, et al. UV light exposure suppresses contact hypersensitivity by abrogating endothelial intercellular adhesion molecule-1 up-regulation at the elicitation site. J Immunol 2003; 171:2855–62.
24. Matsushita Y, Hasegawa M, Matsushita T, Fujimoto M, Horikawa M, Fujita T, et al. Intercellular adhesion molecule-1 deficiency attenuates the development of skin fibrosis in tight-skin mice. J Immunol 2007;179:698–707.
25. Tang ML, Steeber DA, Zhang XQ, Tedder TF. Intrinsic differences in L-selectin expression levels affect T and B lymphocyte subset-specific recirculation pathways. J Immunol 1998;160: 5113–21.
26. Richards H, Longhi MP, Wright K, Gallimore A, Ager A. CD62L (L-selectin) down-regulation does not affect memory T cell distribution but failure to shed compromises anti-viral immunity. J Immunol 2008;180:198–206.
27. Yang S, Liu F, Wang QJ, Rosenberg SA, Morgan RA. The shedding of CD62L (L-selectin) regulates the acquisition of lytic activity in human tumor reactive T lymphocytes. PLoS One 2011;6:e22560.
28. Okiyama N, Sugihara T, Oida T, Ohata J, Yokozeki H, Miyasaka N, et al. T lymphocytes and muscle condition act like seeds and soil in a murine polymyositis model. Arthritis Rheum 2012;64:3741–9.
29. Kogan TP, Dupre B, Bui H, McAbee KL, Kassir JM, Scott IL, et al. Novel synthetic inhibitors of selectin-mediated cell adhesion: synthesis of 1,6-bis[3-(3-carboxymethylphenyl)-4-(2-α-D-mannopyranosyloxy)phenyl]hexane (TBC1269). J Med Chem 1998; 41:1099–111.
30. Beeh KM, Beier J, Meyer M, Buhl R, Zahlten R, Wolff G. Bimosiamose, an inhaled small-molecule pan-selectin antagonist, attenuates late asthmatic reactions following allergen challenge in

mild asthmatics: a randomized, double-blind, placebo-controlled clinical cross-over-trial. Pulm Pharmacol Ther 2006;19:233–41.
31. Friedrich M, Bock D, Philipp S, Ludwig N, Sabat R, Wolk K, et al. Pan-selectin antagonism improves psoriasis manifestation in mice and man. Arch Dermatol Res 2006;297:345–51.
32. Schlag G, Redl HR, Till GO, Davies J, Martin U, Dumont L. Anti-L-selectin antibody treatment of hemorrhagic-traumatic shock in baboons. Crit Care Med 1999;27:1900–7.
33. Seekamp A, van Griensven M, Dhondt E, Diefenbeck M, Demeyer I, Vundelinckx G, et al. The effect of anti-L-selectin (aselizumab) in multiple traumatized patients–results of a phase II clinical trial. Crit Care Med 2004;32:2021–8.
34. Leonardi C, Menter A, Hamilton T, Caro I, Xing B, Gottlieb AB. Efalizumab: results of a 3-year continuous dosing study for the long-term control of psoriasis. Br J Dermatol 2008;158: 1107–16.

DOI 10.1002/art.38622

Clinical Images: Focal myositis demonstrated on positron emission tomography

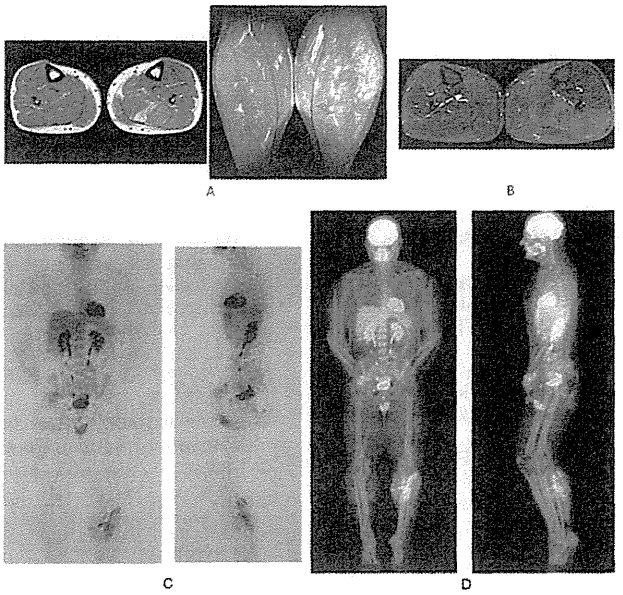

The patient, a 43-year-old man, presented with a 3-month history of pain and swelling involving the posterior part of his left calf, which was exacerbated by palpation. The circumference of the left calf was 3 cm greater than that of the right calf. He denied having any generalized symptoms, including fever, weight loss, or muscle weakness. Laboratory testing revealed elevated levels of creatine phosphokinase (3,470 IU/liter [normal <130 IU/liter]). The results of autoantibody screening tests (rheumatoid factor, antinuclear antibodies, anti–Jo-1, PL-7, PL-12, and anti–signal recognition particle) were negative. The patient had negative findings on serologic tests for infection with cytomegalovirus, Epstein-Barr virus, coxsackievirus, parvovirus, hepatitis virus, human immunodeficiency virus, and *Toxoplasma*. A heterogeneous mass involving the medial head of the left gastrocnemius and soleus muscles was shown on gadolinium-enhanced T1-weighted (**A**) and T2-weighted (**B**) magnetic resonance images. Positron emission tomography (PET) (**C**) and ^{18}F-fluorodeoxyglucose(FDG)–PET scanning (**D**) revealed marked uptake of FDG in the left calf muscles. Histologic assessment of the muscles confirmed the diagnosis of focal myositis, with findings of inflammatory infiltrates associated with necrosis and degeneration/regeneration of muscle fibers. Subsequently, the patient was given prednisone therapy (at an initial dosage of 30 mg/day), which resulted in resolution of the focal myositis. This case supports the notion that FDG-PET scanning is a noninvasive test that is helpful for providing both detailed and complete morphofunctional cartography of muscle changes and guiding muscle biopsy. Thus, when compared with magnetic resonance imaging, FDG-PET scanning has the advantage of showing the absence of other sites of muscle inflammation, which confirms the diagnosis of focal myositis, and excluding underlying malignancy associated with myositis.

Isabelle Marie, MD, PhD
Gaetan Sauvêtre, MD
Stéphanie Becker, MD
Anne-Laure Bedat-Millet, MD
Centre Hospitalier Universitaire Rouen
Rouen, France

CORRESPONDENCE

Anti-MDA5 antibody-positive dermatomyositis with lethal progressive interstitial lung disease and advanced gastric cancer

Dermatomyositis (DM) is an autoimmune inflammatory disease often associated with internal malignancy and interstitial lung disease. The latter is found in about 50% of patients with DM and is a life-threatening complication of the disease [1]. Rapidly progressive interstitial lung disease (RP-ILD) associated with clinically amyopathic dermatomyositis (CADM) is often lethal, despite treatment by corticosteroid therapy combined with immunosuppressive drugs [2].

A number of autoantibodies can be detected in sera of patients with DM, some specific to RP-ILD. Recently, there have been reports that anti-melanoma differentiation-associated gene 5 (MDA5) antibody predicts a fatal outcome in patients with DM complicated by RP-ILD [3]. A close association has been described between the presence of anti-transcription intermediary factor 1γ (anti-TIF-1γ) antibodies and internal malignancy in DM patients [4].

We report a RP-ILD and advanced gastric cancer in a case of anti-MDA5 antibody-positive and anti-TIF-1γ antibody-negative DM. The patient, a 64-year-old Japanese woman, had suffered from photosensitivity, proximal muscle weakness and dyspnea on exertion for the past 4 weeks. Further evaluations, including electromyography, upper endoscopy and thoracoabdominal computed tomography, revealed DM complicated by interstitial lung disease, advanced gastric cancer and paraaortic lymph node swelling. The biopsy specimen from her stomach was positive for poorly-differentiated adenocarcinoma cells. Subsequently, the lung disease progressed rapidly, resulting in a drop of blood oxygenation to a level interfering with her daily activities. At this point, she was referred to our hospital.

Physical examination revealed red-to-violaceous, well demarcated plaques on the face (*figure 1A*), limbs and sacrum. Gottron's papules (*figures 1B-E*), periungual erythema, and nail-fold bleeding on the hands were found. Histopathological examination of skin biopsies from the dorsal interphalangeal joint found hyperkeratosis, atrophy and superficial dermal inflammation with overlying interfacial change (*figure 1F,G*). Laboratory investigations identified increased levels of serum lactate dehydrogenase (611 IU/L), C-reactive protein (5.38 mg/dL), ferritin (1030 ng/mL), creatine kinase (620 IU/L), aldolase (16 U/L), myoglobin (110 ng/mL), carcinoembryonic antigen (28 ng/mL), cancer antigen 19-9 (136 U/mL), KL-6 (1713 U/mL) and surfactant protein-D (105 ng/mL). The oxygen saturation level from a finger probe was 84%, despite the inhalation of oxygen at a rate of 3 L per minute by nasal canula. Arterial blood gas analysis under the same conditions showed mild hypoxia (pH 7.489; PaO_2, 76.2 Torr; $PaCO_2$, 32.3 Torr). Anti-MDA5 antibody was detected by immunoprecipitation [5] and specific enzyme-linked immunosorbent assays.

Intensive therapies, including steroid pulse (1 g/day for 3 days) and cyclosporine (200 mg/day), were administered after the diagnosis of RP-ILD as a complication. These therapies did not improve her respiratory status and the serum muscular enzyme levels decreased. Meanwhile, serum ferritin levels were markedly elevated. At 31 days after admission, she died due to respiratory failure, without starting the treatment for advanced gastric cancer (*figure 1H*).

Although we knew there were anti-MDA5 autoantibodies present, the clinical course of the interstitial lung disease progression was too rapid to rescue. Anti-MDA5 antibody has been described as specific in patients with DM [6], and patients with this autoantibody have no or only mild muscular symptoms compared to patients with typical DM. The specific phenotype of palmar papules and cutaneous ulcerations is associated with this autoantibody in adult DM patients [7]. Our case had moderate muscular symptoms and palmar papules and it is noteworthy that the patient's respiratory status declined, while her muscular symptoms actually improved. Thus, we should pay close attention to respiratory status in DM patients who are anti-MDA5 autoantibody-positive.

Another feature in this case was that the serum ferritin level was elevated in parallel with exacerbation of the respiratory status. Ferritin, an iron-binding protein, regulates iron storage and homeostasis, as well as proinflammatory cytokine signaling [8]. Recently, high levels of ferritin have been associated with the development and prognosis of RP-ILD in patients with DM [9].

We report a rare case of RP-ILD and advanced gastric cancer in a patient with anti-MDA5 antibody-positive DM. Scrupulous attention to lethal RP-ILD must be given to patients with typical DM, even when complicating muscular disease has shown improvement. The DM patient described here, whose respiratory status was exacerbated in parallel with gradual rise of serum ferritin levels under combined modality therapy, is a dramatic clinical example of this need. ■

doi:10.1684/ejd.2014.2381

To cite this article: Yamaoka T, Doi C, Yokomi A, Tanemura A, Murota H, Tani M, Saruban H, Hamaguchi Y, Fujimoto M, Katayama I. Anti-MDA5 antibody-positive dermatomyositis with lethal progressive interstitial lung disease and advanced gastric cancer. *Eur J Dermatol* 2014 (epub ahead of print) doi:10.1684/ejd.2014.2381

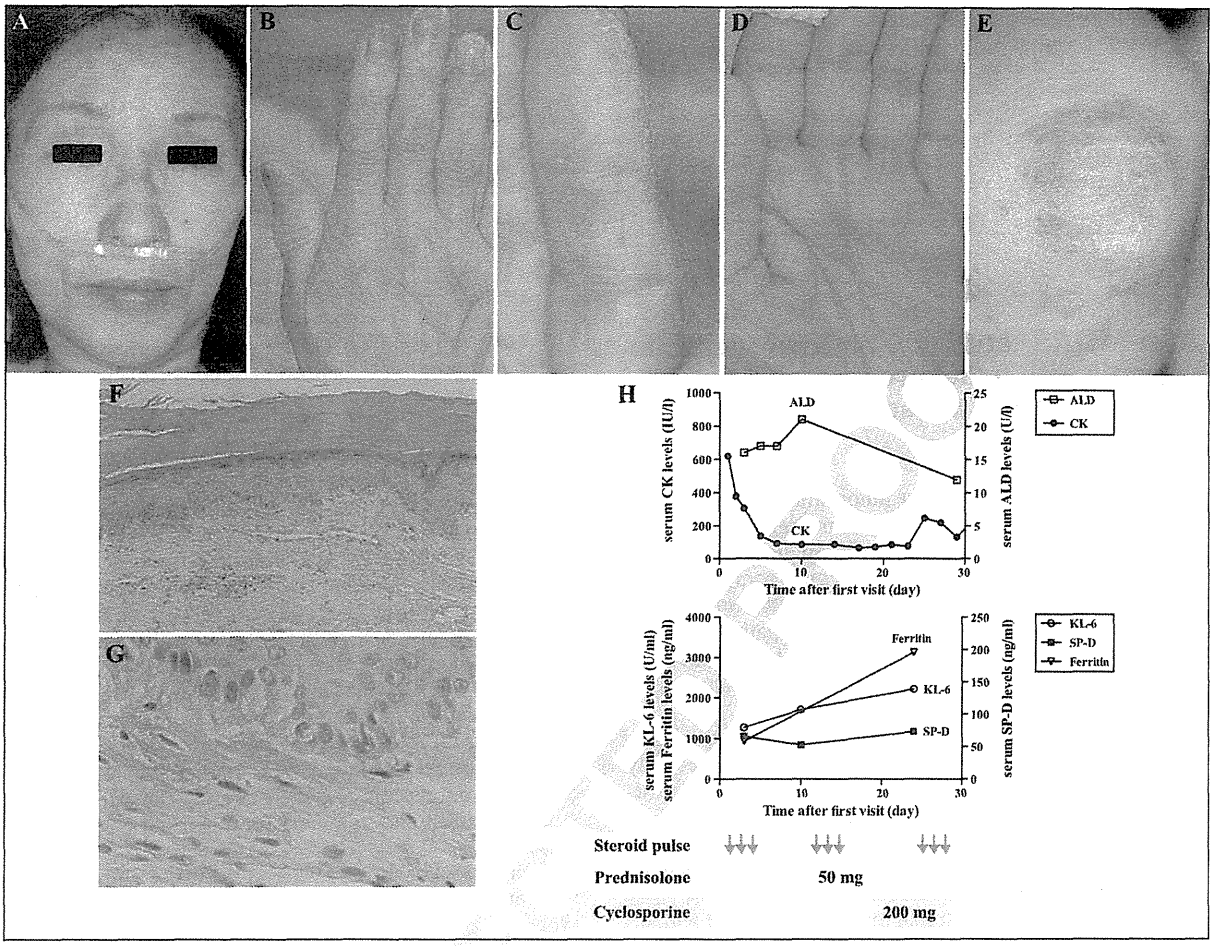

Figure 1. Clinical and histopathological findings, time course of medical treatments, and changes in laboratory data, before and after treatment. **A)** Skin lesions of the face, showing facial erythema with heliotrope rash. **B-E)** Discrete red-purple papules and/or erythematous macules appearing over the dorsal aspect of fingers, palms, and elbows. **F, G)** An atrophic epidermis with hyperkeratosis shows marked vacuolar alteration of basilar keratinocytes, associated with a sparse lymphocytic infiltration around superficial dermal vessels. **H)** Correlation between levels of serum markers and treatment with high-dose methylprednisolone (1 g/day intravenously for 3 days) and cyclosporine (5 mg/kg/day). It is important to note that levels of the muscle marker creatine kinase (CK) showed a gradual reduction, while those of the marker of interstitial lung disease, KL-6, increased. Hematoxylin and eosin staining; magnification in (F) ×40, and in (g) ×400.

Disclosure. *Financial support: none. Conflict of interest: none.*

[1] Department of Dermatology, Osaka University Graduate School of Medicine, 2-2 Yamadaoka, Suita, Osaka 565-0871, Japan
[2] Department of Dermatology, Higashiosaka City General Hospital, Osaka, Japan
[3] Department of Dermatology, Kanazawa University Graduate School of Medical Science, Kanazawa, Japan
<Yamaoka@derma.med.osaka-u.ac.jp>

Toshifumi YAMAOKA[1]
Chie DOI[1]
Akinori YOKOMI[1]
Atsushi TANEMURA[1]
Hiroyuki MUROTA[1]
Mamori TANI[1]
Hiroko SARUBAN[2]
Yasuhito HAMAGUCHI[3]
Manabu FUJIMOTO[3]
Ichiro KATAYAMA[1]

1. Marie I, Hachulla E, Cherin P, *et al.* Interstitial lung disease in polymyositis and dermatomyositis. *Arthritis rheum* 2002; 47: 614-22.

2. Tsuchiya H, Tsuno H, Inoue M, *et al.* Mycophenolate mofetil therapy for rapidly progressive interstitial lung disease in a patient with clinically amyopathic dermatomyositis. *Mod Rheumatol* 2014; EarlyOnline: 1-3.

3. Sato S, Hoshino K, Satoh T, *et al.* RNA helicase encoded by melanoma differentiation-associated gene 5 is a major autoantigen in patients with clinically amyopathic dermatomyositis: Association with rapidly progressive interstitial lung disease. *Arthritis Rheum* 2009; 60: 2193-200.

4. Fujimoto M, Hamaguchi Y, Kaji K, *et al.* Myositis-specific anti-155/140 autoantibodies target transcription intermediary factor 1 family proteins. *Arthritis Rheum* 2012; 64: 513-22.

5. Kaji K, Fujimoto M, Hasegawa M, *et al.* Identification of a novel autoantibody reactive with 155 and 140 kDa nuclear proteins in patients with dermatomyositis: an association with malignancy. *Rheumatology* 2007; 46: 25-8.

6. Sato S, Hirakata M, Kuwana M, *et al.* Autoantibodies to a 140-kd polypeptide, CADM-140, in Japanese patients with clinically amyopathic dermatomyositis. *Arthritis Rheum* 2005; 52: 1571-6.

7. Fiorentino D, Chung L, Zwerner J, Rosen A, Casciola-Rosen L. The mucocutaneous and systemic phenotype of dermatomyositis patients with antibodies to MDA5 (CADM-140): a retrospective study. *J Am Acad Dermatol* 2011; 65: 25-34.

8. Kwak EL, Larochelle DA, Beaumont C, Torti SV, Torti FM. Role for NF-kappa B in the regulation of ferritin H by tumor necrosis factor-alpha. *J Biol Chem* 1995; 270: 15285-93.

9. Gono T, Sato S, Kawaguchi Y, *et al.* Anti-MDA5 antibody, ferritin and IL-18 are useful for the evaluation of response to treatment in interstitial lung disease with anti-MDA5 antibody-positive dermatomyositis. *Rheumatology* 2012; 51: 1563-70.

doi:10.1684/ejd.2014.2381

Acta Derm Venereol 2014; 94: 478–479

SHORT COMMUNICATION

Pemphigus Foliaceus Associated with Anti-NXP2 Autoantibody-positive Dermatomyositis

Noriki Fujimoto[1], Satoru Takayama[1], Yasuhito Hamaguchi[2], Manabu Fujimoto[2] and Toshihiro Tanaka[1]

Departments of Dermatology, [1]Shiga University of Medical Science, Setatsukinowa, Otsu, Shiga 520-2192, and [2]Faculty of Medicine, Institute of Medical, Pharmaceutical and Health Sciences, Kanazawa University, Ishikawa, Japan. E-mail: noriki@belle.shiga-med.ac.jp

Accepted Sep 3, 2013; Epub ahead of print Nov 11, 2013

Pemphigus foliaceus (PF) is one of the autoimmune blistering diseases (ABDs) characterised by autoantibodies (Abs) binding to desmoglein (Dsg) 1, resulting in acantholysis and intraepidermal blistering. Several other autoimmune diseases have been reported to occur in patients with ABDs, such as rheumatoid arthritis, systemic lupus erythematosus, and Grave's disease (1). However, ABD associated with dermatomyositis (DM) is rare. We report here the first case in which the Ab of DM is identified.

CASE REPORT

A 39-year-old Japanese woman with a 4-month history of skin eruptions was referred to our hospital in July 2007. Physical examination showed pruritic malar erythema on the face, including the medial canthi of the eyes and alar part of the nose (Fig. 1A), diffuse alopecia and erythema on the scalp, and Gottron's papules on the dorsum of the hands (Fig. 1B). Muscle weakness and dysphagia were not present, and cutaneous calcinosis was not found. She had no medical history of note. A biopsy specimen from the erythematous lesion on the cheek showed mild basal vacuolar change and sparse superficial perivascular infiltration of lymphocytes. Direct immunofluorescence microscopy revealed no deposition of immunoglobulin or complement. Laboratory investigations showed raised levels of creatine kinase (514 IU/l; normal 45–163) and aldolase (10.7 IU/l; 2.1–6.1). Circulating Abs against Jo-1, SS-A/Ro, and SS-B/La were not detected using enzyme-linked immunosorbent assay (ELISA). Anti-nuclear matrix protein 2 Ab (anti-NXP2 Ab) was identified by immunoprecipitation assay with 35S-labelled K562 cell extracts (2). Biopsy from the left quadriceps femoris muscle showed no apparent findings of myositis. We diagnosed the patient with clinically amyopathic dermatomyositis (CADM). Screening for internal malignancy and interstitial lung disease was negative. We treated the patient with topical, not systemic, corticosteroids. The skin eruptions of DM gradually improved from April 2008 and had almost disappeared in June 2009. Anti-NXP2 Ab was no longer detected in the sera in June 2011, and DM has not relapsed for 3 years.

In December 2009, she noticed mild erythema on the chest and back. She presented with some erythema and erosions on the chest and back (Fig. 1C) in June 2010. There was no mucous membrane involvement. Histopathological examination of a biopsy specimen showed acantholysis and superficial split in the granular layer (Fig. 1D). Direct immunofluorescence showed intercellular staining for IgG and C3 in the epidermis. Anti-Dsg Ab ELISA was positive for anti-Dsg 1 (index value: 146; cut-off: 14) but negative for anti-Dsg 3. Based on these results, PF was diagnosed. ELISA for anti-Dsg 1 and Dsg 3 was retrospectively examined for the serum extracted in 2007, and results was negative. The patient refused to use systemic steroids. Complete remission has not been achieved using topical corticosteroids. However, the clinical severity of PF has been stable, and the index value of anti-Dsg1 Ab by ELISA has been around 40.

DISCUSSION

To date, there are only 6 cases of ABD including our case reported in the English literature (3–7) (Table SI[1]).

[1]http://www.medicaljournals.se/acta/content/?doi=10.2340/00015555-1756

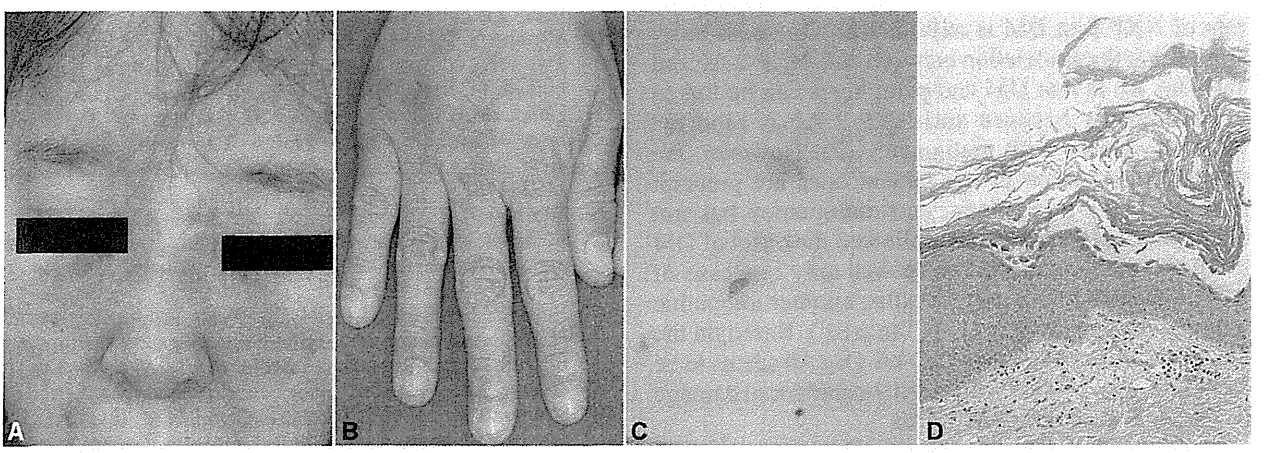

Fig. 1. (A, B) Clinical presentation of dermatomyositis at initial appearance in July 2007. (A) Pruritic malar erythema on the face, including the medial canthi of the eyes and alar part of the nose. (B) Gottron's papules on the dorsum of the right hand. (C) Clinical presentation of pemphigus foliaceus (PF) in June 2010. Mild erythema and erosions were observed on the back. (D) Histopathological findings of erythematous lesion of PF (H&E, original magnification ×200). Acantholysis and superficial split in the granular layer were observed.